

## On a new *Melanosuchus* species (Alligatoroidea: Caimaninae) from Solimões Formation (Eocene-Pliocene), Northern Brazil, and evolution of Caimaninae

JONAS PEREIRA DE SOUZA-FILHO<sup>1,2\*</sup>, EDSON GUILHERME<sup>1,3</sup>, PETER MANN DE TOLEDO<sup>5</sup>, ISMAR DE SOUZA CARVALHO<sup>6</sup>, FRANCISCO RICARDO NEGRI<sup>7</sup>, ANDRÉA APARECIDA DA ROCHA MACIENTE<sup>1,4</sup>, GIOVANNE M. CIDADE<sup>8</sup>, MAURO BRUNO DA SILVA LACERDA<sup>9</sup> & LUCY GOMES DE SOUZA<sup>10\*</sup>


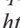
<sup>1</sup>Laboratório de Pesquisas Paleontológicas (LPP), Centro de Ciências Biológicas e da Natureza, Universidade Federal do Acre, BR 364, Km 04, 69.920-900, Rio Branco, Acre, Brazil.

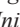

<sup>2</sup> [jpdessouza filho@hotmail.com](mailto:jpdessouza filho@hotmail.com);  <https://orcid.org/0000-0003-0481-3204>

<sup>3</sup> [guilherme.edson@gmail.com](mailto:guilherme.edson@gmail.com);  <https://orcid.org/0000-0001-8322-1770>



<sup>4</sup> [andreamaciente@gmail.com](mailto:andreamaciente@gmail.com);  <https://orcid.org/0000-0003-3504-1833>

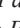

<sup>5</sup>INPE—Instituto Nacional de Pesquisas Espaciais, MCT, São José dos Campos, São Paulo, Brazil.

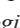

 [peter.toledo@hotmail.com](mailto:peter.toledo@hotmail.com);  <https://orcid.org/0000-0003-4265-2624>

<sup>6</sup>Departamento de Geologia, CCMN-IGEO, Universidade Federal do Rio de Janeiro, 21.910-200, Cidade Universitária—Ilha do Fundão, Rio de Janeiro, Rio de Janeiro, Brazil.  [ismar@geologia.uff.br](mailto:ismar@geologia.uff.br);  <https://orcid.org/0000-0002-1811-0588>



<sup>7</sup>Laboratório de Paleontologia, Universidade Federal do Acre—Campus Floresta, 69895-000, Cruzeiro do Sul, Acre, Brazil.

 [frnegri@bol.com.br](mailto:frnegri@bol.com.br);  <https://orcid.org/0000-0001-9292-7871>

<sup>8</sup>Laboratório de Estudos Paleobiológicos, Departamento de Biologia, Universidade Federal de São Carlos—Campus Sorocaba, 13052-780, Sorocaba, São Paulo, Brazil.  [giovannecidade@hotmail.com](mailto:giovannecidade@hotmail.com);  <https://orcid.org/0000-0001-8621-5122>

<sup>9</sup>Pós-Graduação em Zoologia, Departamento de Zoologia, Instituto de Ciências Biológicas, Universidade Federal de Minas Gerais, 31270-901, Belo Horizonte, Minas Gerais, Brazil.  [mauro.lacerda.bio@gmail.com](mailto:mauro.lacerda.bio@gmail.com);  <https://orcid.org/0000-0002-8403-7884>

<sup>10</sup>Museu da Amazônia, Margarita 6305, Jorge Teixeira, 10795-265, Manaus, Amazonas, Brazil.

 [souzalucyg@gmail.com](mailto:souzalucyg@gmail.com);  <https://orcid.org/0000-0003-2819-7776>

\*Corresponding authors

### Abstract

The Solimões Formation (Eocene-Pliocene) is a well-known geological unit due to the great diversity of crocodylian species. Here we describe a new species of *Melanosuchus*, *M. latrubessei* **sp. nov.**, from the Talismã locality, state of Amazonas, from the Upper Miocene of the Solimões Formation (Solimões Basin, Brazil). A new phylogenetic inference focused on Caimaninae is provided and the different evolutionary scenarios involving this new species are discussed. In addition, quantitative morphology studies are carried out and comments regarding the paleoecology aspects of this new species are made. *M. latrubessei* represents a medium-sized generalist predator, being proportional to the medium-sized *M. niger*. This new species inhabited the drainages of the Solimões Formation and was ecologically related to other taxa of crocodylians during the proto-Amazon Miocene. The evolutionary advantages of *Melanosuchus* genus are discussed to better understand the biogeographical occurrence of *M. niger* in South America, a species which survives to this day in contrast to several other species that became extinct during the Miocene-Pliocene periods. The extinction of the Miocene-Pliocene crocodylian taxa of the Solimões Formation, including *Melanosuchus latrubessei*, seems to be directly related with the uplift of the northern portions of the Andes, which generated significantly changes in drainages and Amazon paleoenvironments.

**Key words:** Crocodylia, Miocene, Neogene, Proto-Amazon, Solimões Basin

### Introduction

The occurrence of fossil vertebrates, plants and mollusks from southwestern regions of the Brazilian Amazon has been recorded since the 19<sup>th</sup> century (e.g. Chandless 1866; Gervais 1876; Barbosa-Rodrigues 1892; for further information, see Rancy 1985; Souza-Filho & Guilherme 2015). Throughout the 20<sup>th</sup> century, sporadic collection and fieldwork efforts were made in this region, aiming at improving the knowledge about geomorphology and fossil occurrences, which culminated in the creation of paleontological collections from materials proceeding from this

region (e.g. Price 1967; Campos *et al.* 1976; Price *et al.* 1977). However, it was only in the 1980's, with the institutionalization of paleontological activities at the Universidade Federal do Acre, that studies on the fossil biodiversity of the North of Brazil began to be produced and published (Souza-Filho & Guilherme 2015). Most of these discoveries are related to the rocks from the uppermost portion of the Solimões Formation, Neogene of the Acre and Solimões Basins, which are assigned to the Upper Miocene (Huayquerian mammal age, ~9 - 6.5 Ma; Latrubesse *et al.* 1997, 2007, 2010; Bissaro-Júnior *et al.* 2019). The deposition of sediments in this Formation is related to the Andean origin (Horbe *et al.* 2019), and is extremely important for understanding the origin of the current Amazonian hydrographic basin and the evolution of the associated fauna and flora during the early Cenozoic (Cozzuol 2006; Hoorn *et al.* 2010, 2017; Latrubesse *et al.* 2007, 2010).

The Solimões Formation have provided countless specimens of a great diversity of clades, such as fish, lizards, snakes, crocodylians, turtles, birds and mammals (Cozzuol 2006), thus demonstrating the scientific potential and the historical importance of this formation to understanding the evolution of the South American paleofauna (Haag & Henriques 2016). In particular, the crocodylian clade presents a high diversity of species with a wide variety of sizes, habits and skull shapes (Riff *et al.* 2010; Souza-Filho *et al.* 2014; Souza *et al.* 2016; Cidade *et al.* 2019a). Nowadays, the Solimões Formation comprises at least seven Crocodyliformes species formally described, namely: *Acosuchus pachytemporalis* Souza-Filho *et al.* 2019; *Charactosuchus fieldsi* Langston 1965 (Souza-Filho 1993); *Brasilotosuchus mendesi* (Souza-Filho & Bocquentin-Villanueva 1989); *Caiman brevirostris* Souza-Filho 1987; *Gryposuchus jessei* Gürich 1912; *Mourasuchus amazonensis* Price 1964; *Mourasuchus arendsi* Bocquentin-Villanueva 1984; and *Purussaurus brasiliensis* Barbosa-Rodrigues 1892. However, there are also some generic records that have not yet been formally described, such as *Charactosuchus* sp. and *Hesperogavialis* sp. (see Riff *et al.* 2010) in addition to other materials that are described into broader systematic categories (e.g. Souza *et al.* 2016; Lacerda *et al.* 2020).

Many of the aforementioned Crocodyliformes genera have also been described from other Cenozoic geological strata of the South America, such as the Urumaco Formation (Venezuela), Honda Group (Colombia) and Ituzaingó Formation (Argentina) (Cozzuol 2006). Regarding this crocodylian fauna, we highlight that the Solimões and Urumaco Formations share the following genera: *Caiman*, *Charactosuchus*, *Gryposuchus*, *Hesperogavialis*, *Mourasuchus* and *Purussaurus* (Aguilera 2004; Aguilera, *et al.* 2006; Riff & Aguilera 2008; Scheyer & Moreno-Bernal 2010; Souza-Filho *et al.* 2014; Cidade *et al.* 2017; Scheyer *et al.* 2019), while the Honda Group and Solimões Formation share the genera: *Caiman*, *Charactosuchus*, *Gryposuchus*, *Mourasuchus* and *Purussaurus* (Langston 1965; Riff *et al.* 2010), and the Ituzaingó Formation shares with Solimões Formation the genera: *Caiman*, *Gryposuchus* and *Mourasuchus* (Gasparini 1968; Langston & Gasparini 1997; Bona *et al.* 2013a, 2017a; Cidade *et al.* 2019a), and such shared faunas provide clues about biogeography and evolutionary history in South America.

Despite the faunal similarities aforementioned, the fossil record of *Melanosuchus* genus is restricted to the late Miocene of Urumaco Formation (Medina 1976; Riff *et al.* 2010; Scheyer & Delfino 2016; Bona *et al.* 2017b; Foth *et al.* 2017; Cidade *et al.* 2019a) and to the Eocene-Pliocene from Solimões Formation (Lacerda *et al.* 2020), being the latter a partial tibia referred to *Melanosuchus* cf. *M. niger*, which represents the first postcranial material of the genus from Solimões Formation (Lacerda *et al.* 2020). The Urumaco Formation occurrence refers to the former *Melanosuchus fisheri* Medina 1976, which nowadays is considered as *nomen dubium* (*sensu* Bona *et al.* 2017b). The holotype of *M. fisheri* (MCNC 243) was referred to *Melanosuchus* sp. (Bona *et al.* 2017b), and to *Melanosuchus* cf. *M. niger* (Foth *et al.* 2017), while the referred specimen (MCZ 4336) was later considered as a *Globidentosuchus brachyrostris* Scheyer *et al.* 2013 (see Bona *et al.* 2017b; Foth *et al.* 2017). In addition, there is also a skull with an associated mandible that was originally referred to *M. fisheri* (AMU-CURS-234; Scheyer & Delfino 2016); however, Bona *et al.* (2017b) assigned this specimen as *Melanosuchus* sp.

Concerning to the extant *Melanosuchus niger* (Spix 1825), this species has a wide distribution along Northern South America (Bolivia, Brazil, Colombia, Ecuador, French Guiana, Guyana, Peru, and Venezuela [unconfirmed] *sensu* Grigg & Kirshner 2015; see also Thorbjarnarson 2010) and represents an important component of the Amazon biome. This wide temporal interval between the fossil record and the extant species of *Melanosuchus* leaves some puzzling questions, such as: (1) the phylogenetic relationship; filling in this gap will enable us to acquire new information regarding the origin and fixation of the specific and supra-specific features; (2) the temporal and spatial distribution; to understand the biogeographical history of *Melanosuchus*; and (3) the reason for the persistence of *M. niger*; which were the natural selection forces and the features that enabled it to survive and occupy an important niche of top predator nowadays (Thorbjarnarson 2010; Grigg & Kirshner 2015), while several other contemporary crocodylian species were extinct.

Intending to offer clues on the issues raised, this work provides the description of a new species of *Melanosuchus*, representing the first cranial record of the genus from Solimões Formation (Upper Miocene). This new species provides key information that allows a better understanding of morphological features shared with the extant *M. niger*, and new interpretations related to the biogeographical and temporal distribution of the *Melanosuchus* species. In addition, comparisons of the rostral shape were carried out through multivariate analyses and inferences about the paleoecology of this new species, comparing the main features that underlie the paleoecological discussions related to *M. latrubessei* during the Miocene, were made. Finally, this paper discusses the evolution of Caimaninae considering the new evidence that is presented here.

### ***Melanosuchus* and its prolific debates**

*Melanosuchus* was originally proposed by Gray (1862) as a monospecific genus to relocate the species *Caiman niger* described by Spix (1825). For a synonym list of *Melanosuchus niger* see Medem (1963). Regarding the phylogenetic relationships of the genus there are two main propositions: 1) nested within *Caiman* genus, frequently as sister of *C. latirostris* (e.g., Poe 1996; Brochu 1997, 1999; Souza-Filho *et al.* 2019); or, 2) as sister species of *Caiman* genus (e.g., Oaks 2011; Roberto *et al.* 2020). The validity of the *Melanosuchus* is still an open debate with some authors suggesting its synonymization with *Caiman* (Poe 1996), this discussion, for now, goes beyond the scope of the present contribution. However, we suggest that the propositions made by Fitzhugh (2016) for molecular inferences should be considered in future works addressing this question.

### **Geological background**

The Solimões Formation is a controversial geological unit, with open debates about its distribution, stratigraphic composition, paleoenvironmental interpretation and age (see Latrubesse *et al.*, 2010; and Souza *et al.* 2016). In Brazil, this formation is situated within the States of Acre and Amazonas, in the North region, being also exposed in east of Peru and north of Bolivia (Duarte 2011). Latrubesse *et al.* (2010) described the rocks of the Solimões Formation as composed mainly by claystones, with calcareous concretions, calcite and gypsum veins, lying in horizontal to sub-horizontal beds, reaching a thickness of over 1,000 m. Here we interpret the Solimões Formation as being predominantly floodplain-lacustrine-swampy (*sensu* Latrubesse *et al.* 2010) with its sedimentary deposition occurring in a dynamic paleoenvironment of shallow lakes and swamps interconnected by a fluvial system of Andean origin (Hoorn *et al.* 2010).

Regarding the age, we consider the temporal range Eocene-Pliocene for the formation as a whole (*sensu* Cunha 2007). However, some outcrops are traditionally considered as Upper Miocene, based on biochronology established through the correlation between tetrapod's and palynology with other regions of South America (see Cozzuol 2006; Kerber *et al.* 2017; Latrubesse *et al.* 1997, 2007, 2010; Negri *et al.* 2010; Ribeiro *et al.* 2013). The Talismã locality (outcrop in the southern region of the State of Amazonas), specifically, where the *Melanosuchus latrubessei* **sp. nov.** was collected, has a radioisotopic dating via U-Pb detrital zircon ( $10.89 \pm 0.13$  Ma; Bissaro-Júnior *et al.* 2019). This age indicates that the Talismã outcrop had its geological strata formed at the maximum deposition in the Tortonian age, late Miocene (Bissaro-Júnior *et al.* 2019). However, as the age of the detritic zircon is related to genesis of the rocks, the age of the locality must be necessarily less than the values acquired, as it must be considered weathering in the matrix rock, transport and deposition of the sediments that originated the studied sedimentary rocks (see Fedo *et al.* 2003). In addition, no stratigraphic correlation was established between the two fossiliferous strata described by Cozzuol (2006) with the locality presenting three localities studied by Bissaro-Júnior *et al.* (2019) in this dating approach. However, regardless of that, the late Miocene age is in agreement with previous biochronological data (Cozzuol 2006; Latrubesse *et al.* 2007, 2010; Bissaro-Júnior *et al.* 2019).

### **Material and methods**

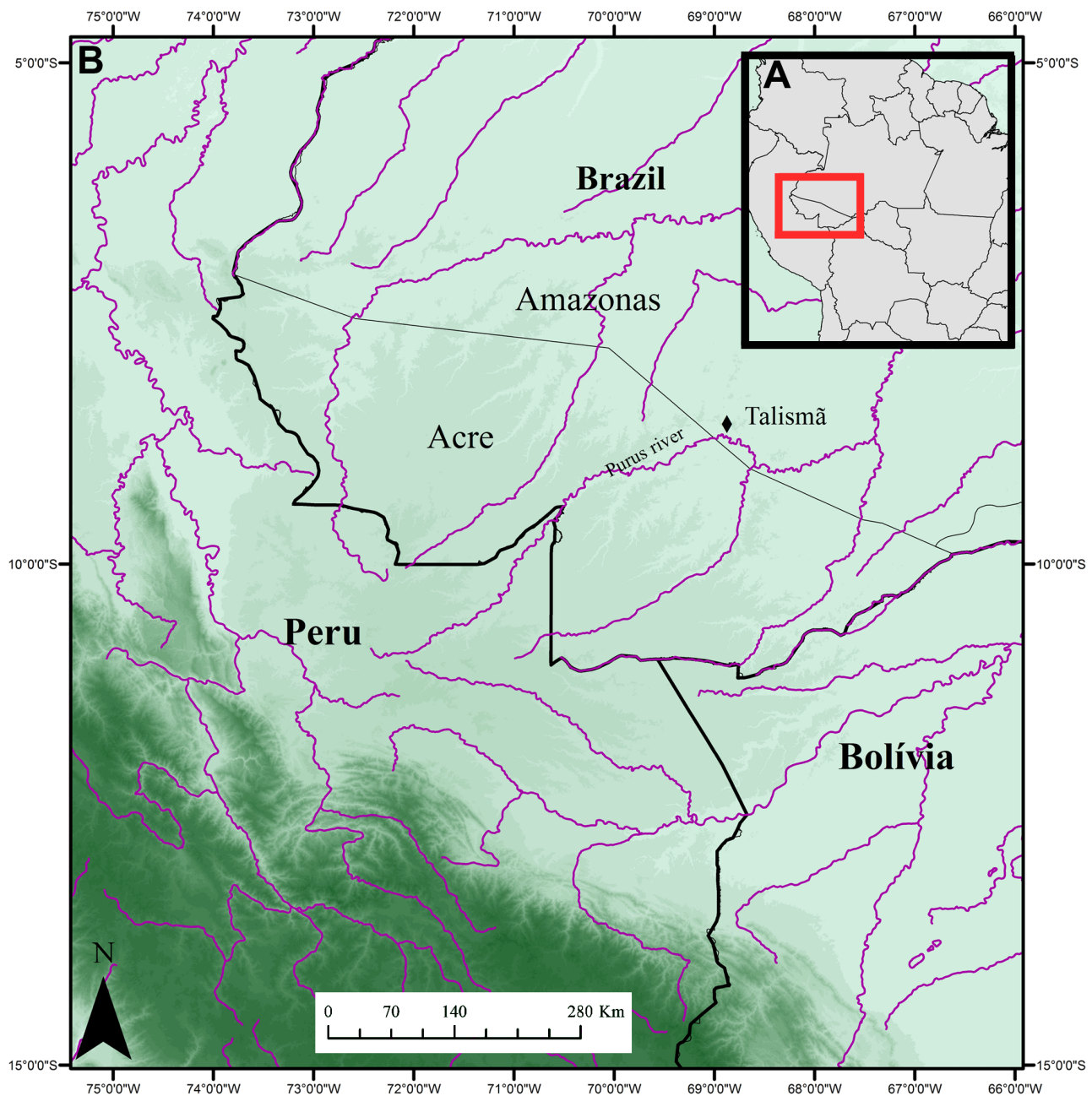
*Institutional abbreviations.* **AMNH**—American Museum of Natural History, New York, United States; **DGM**—Divisão de Geologia e Mineralogia, Museu de Ciências da Terra, Brazilian Geological Survey, Rio de Janeiro, Brazil; **FMNH**—Field Museum of Natural History, Chicago, United States; **LPP**—Laboratório de Pesquisas Paleontológicas da UFAC, Rio Branco, Brazil; **MCNC**—Museo de Ciencias Naturales de Caracas, Caracas, Venezuela; **MCZ**—Museum of Comparative Zoology, Cambridge, United States; **MLP**—Museo de La Plata, La Plata, Argentina; **MNRJ**—Museu Nacional, Universidade Federal do Rio de Janeiro, Rio de Janeiro, Brazil; **MUSM**—Natural His-



tory Museum of San Marcos University, Lima, Peru; **MZUSP**—Museu de Zoologia da Universidade de São Paulo, São Paulo, Brazil; **SMF**—Senckenberg Museum, Frankfurt, Germany; **UCMP**—University of California Museum of Paleontology, Berkeley, United States; **UF**—University of Florida, Gainesville, United States; **UFAC**—Universidade Federal do Acre, Rio Branco, Brazil; **ZS**—Zoologische Staatssammlung, Munich, Germany.

### Fossiliferous locality and new specimen

The new species described in this work is based on the specimen UFAC 2793, which consists on a nearly complete rostrum (i.e. premaxilla and maxilla) from the right half of the skull. The specimen was collected in 1995 at the Talismã outcrop, located at the right margin of the upper Purus River in southern part of the Amazonas State, Brazil (08°46'37,8"S; 68°54'15,1"W; Figure 1), and is housed in the paleovertebrates collection of the Laboratório de Pesquisas Paleontológicas (LPP) of the Universidade Federal do Acre, in Rio Branco, State of Acre. The precise facies where the fossil was found could not be properly determined.



**FIGURE 1.** Localization of the Talismã fossiliferous outcrop, State of Amazonas, Brazil. (A) Indication of the locality in a South America map (red rectangular box); and, (B) The red rectangular box, in zoom, with a black prism indicating the Talismã locality.



## Morphological comparisons and phylogenetic inference

In the morphological comparisons, several individuals of extant Caimaninae species were studied (see details in Table 1). Furthermore, aiming for a proper comparison of the vomer and related bones in *M. niger*, the specimens UFAC R-98 and UFAC R-203 had the vomer disarticulated.

**TABLE 1.** List of *Jacarea* (at least *a priori*) specimens from extant and fossil species used for comparisons. Legends: (?), dubious identification; \*, holotype; **bold**, specimens personally studied; underlined, specimens studied by photos/bibliography.

Species	Specimens	Bibliography
<i>Caiman brevirostris</i>	UFAC 196* and UFAC 5388	Souza-Filho (1987) and Fortier <i>et al.</i> (2014)
<i>Caiman crocodilus</i>	AMNH R 73048; AMNH R 137179; DGM 155 RR; DGM 300 RR; MNRJ 1030; MZUSP-C 2014; MZUSP-C 2063; MZUSP-C 2113; UF 45439; UFAC R-140; UFAC R-191 and USNM 313860	-
<i>Caiman gasparinae</i>	MLP-73-IV-15-1* and MACN PV 5555	Bona & Carabajal (2013)
<i>Caiman latirostris</i>	AMNH R 143183; DGM 153-RR; DGM 156-RR; MNRJ 1445; MZUSP-C 2137; UF 99046 and UF 99223	-
<i>Caiman lutescens</i> (?)	UCMP 39978	Langston (1965) and Bona <i>et al.</i> (2013a,b); Bona & Barrios (2015)
<i>Caiman yacare</i>	AMNH R 97305; AMNH R 97334; AMNH R 120028; MNRJ 25437; MNRJ 25460; MZUSP-C 2138 and MZUSP-C 2140	-
<i>Caiman wannlangstoni</i>	<u>MUSM 2377*</u>	Salas-Gismondi <i>et al.</i> (2015)
<i>Melanosuchus fisheri</i> (?)	MCNC 243* and <u>AMUCURS-234</u>	Medina (1976) and Bona <i>et al.</i> (2017)
<i>Melanosuchus niger</i>	AMNH R 58130; AMNH R 101419; FMNH 45653; MCT 286-RR; MN 61; MN 63; MN 64; MN 66; MN 81; MN 3174; MZUSP-C 2428; SMF 30102; SMM 30113; UF 62641; UF 72914; UF 1045123; UFAC R-018; UFAC R-98; UFAC R-136; UFAC R-203; UFAC R-207; UFAC R-474; UFAC s/ n° A; UFAC s/n° B; USNM 257785; ZS 3; ZS 11; ZS 13; ZS 14; ZS 46; ZS 52; ZS 57; ZS 64; ZS 69; ZS 75; ZS 77; ZS 79; and ZS 89.	-
<i>Paleosuchus palpebrosus</i>	UFAC R-215	-

The phylogenetic analysis was performed based on the phylogenetic matrix of Souza-Filho *et al.* (2019), which is mainly based on the matrix of Brochu (2011). The matrix has 94 taxa, being 93 eusuchian taxa in the ingroup and the neosuchian crocodyliform *Bernissartia fagesii* Dollo 1883 as an outgroup and 187 morphological characters (morphological data matrix is available in SI 2; and the list of morphological characters is available on SI 4). Additionally, *Melanosuchus latrubessei* **sp. nov.** was included in the data matrix, while *M. fisheri* was excluded (as it is considered a *nomen dubium* following Bona *et al.* 2017b). Despite this, information about the holotype of *M. fisheri* was included separately in results and discussion, as regardless of being a valid species or not, this specimen would be one of the oldest known for the genus and plays an important role in the understanding of evolution of the genus. The new species was scored using the software Mesquite 3.03 (Maddison & Maddison 2015).

The phylogenetic analysis was performed in the software *Tree analysis using New Technology* (TNT 1.5 -

Goloboff & Catalano 2016). The morphological characters were adjusted as non-additive. We performed a first analysis using new technologies with sectorial search, ratchet and tree fusing (all in default configuration), followed by driven search (initial addsequence [10], find minimum length [50] times, random seed [0], collapse and replace trees). A second analysis, with the trees recovered in the first one was conducted, via traditional search (trees from RAM, stop when max trees hit, swapping algorithm [TBR] and collapse trees after the search). The strict consensus and the common 'synapomorphy' list were obtained and the minimum-length trees (MLT) recovered (available in SI 3). The output of the commands and results obtained from TNT, including the common 'synapomorphy' list and the strict consensus are available in SI 1.

### Shape analysis

In order to explore the morphology of *Melanosuchus latrubessei* **sp. nov.** and compare its rostral shape to that of extant *Melanosuchus*, we performed a two-dimensional geometric morphometrics (GM) analysis, which represents a quantitative method used to describe shape of biological structures, based on a set of anatomical discrete 'points' called landmarks (Slice 2007; Webster & Sheets 2010; Klingenberg 2013; Cooke & Terhune 2015; see also Adams *et al.* 2013 for advances in GM methods).

We performed two distinct analyses using photographs of *M. latrubessei* and 25 specimens of *M. niger*, both from right rostrum. In this analysis, we do not include the specimens of *Melanosuchus* sp. (originally described as *M. fisheri*), considering that images favorable to this type of analysis were not obtained. The first analysis of the dorsal view was performed based on nine landmarks and the second one performed from the ventral view using 10 landmarks. In both views analyzed, the selection of landmarks was based on the preserved structures of the specimen described in this work, thus evaluating the rostral shape of *Melanosuchus*, considering such taphonomic limitations that are discussed below (to details on specimens and landmarks see Table S1, Table S2 and Figure S2, available in SI 1).

The set of images were organized using the software *tpsUtil* 1.76 (Rohlf 2015). The landmarks were digitalized through the software *tpsDig2* 2.31 (Rohlf 2015). The Generalized Procrustes Analysis (GPA), which aims at making the data comparable, removes existing differences between each individual's landmark settings, through the following steps: translation (removing position differences), scaling (removing size differences), and rotation (removing orientation differences) of each individual coordinates (Webster & Sheets 2010; Zelditch *et al.* 2012) was performed using the software *Paleontological Statistics* (PAST 4.01—Hammer *et al.* 2001).

The multivariate data obtained were explored through Principal Component Analysis (PCA), a method that orthogonally organizes the original variables in a new set of variables in a smaller number of dimensions in a Cartesian plane composed of axes of morphological variance (i.e. Principal Components - PCs), allowing the projection of the data and facilitating the visualization of the individuals' morphological variance (Hammer & Harper 2008; Webster & Sheets 2010; Zelditch *et al.* 2012). The PCA analyses were performed using the software PAST (Hammer *et al.* 2001) and the summarized morphological variance were visualized in the software *tpsRelw* (Rohlf 2015). The PCs that showed the greatest significance were interpreted and illustrated in the manuscript. The broken stick model detailed in Jackson (1993) was used to define the described PCs. According to Monteiro (2013) the percentage of variance explained by each component is compared with a null distribution of expected percentages, when the variation total is randomly distributed among the PCs (see Jackson 1993; and Monteiro 2013 for further information on broken stick). We also explored the transformation grids, or thin-plate splines (TPS) that allows to visualize changes in shape (Zelditch *et al.* 2012; Klingenberg 2013) from *tpsRelw* (Rohlf 2015); such grids help in later descriptions of variation of the shape.

## Results

### Systematic Paleontology

CROCODYLIA Gmelin 1789 (*sensu* Benton & Clark 1988)

BREVIROSTRES Zittel 1890

ALLIGATOROIDEA Gray 1844 (*sensu* Norell, Clark & Hutchison 1994)

ALLIGATORIDAE Cuvier 1807

CAIMANINAE Brochu 1999

JACAREA Gray 1844 (*sensu* Brochu 1999)

*Melanosuchus* Gray 1862

**Type-species:** *Melanosuchus niger* (Spix 1825) (see Hoogmoed & Gruber 1983 for type specimens)

***Melanosuchus latrubessei* sp. nov.**

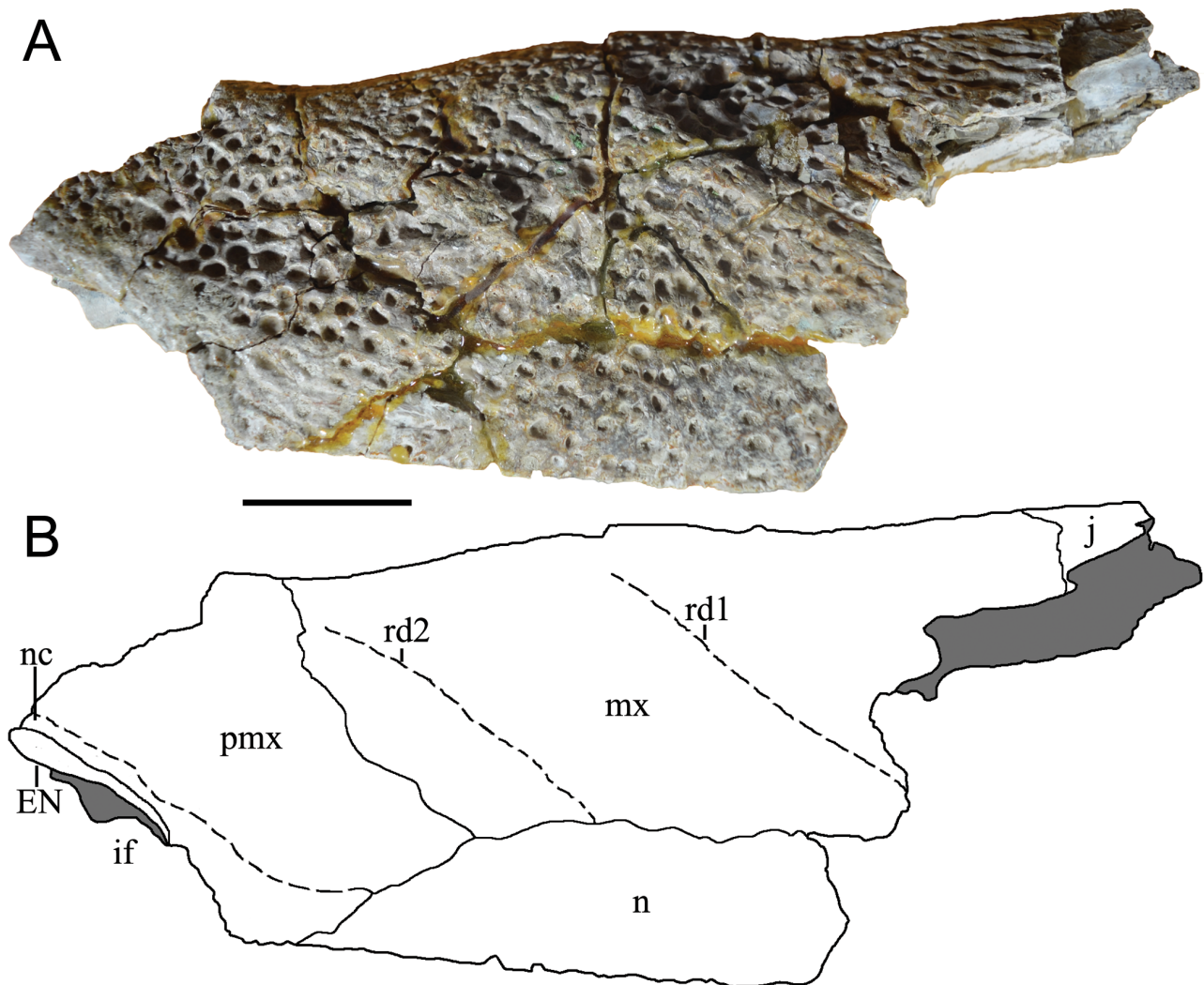
(Figure 2, 3, 4, 5 and 6)

Zoobank species: urn:lsid:zoobank.org:act:BB6E5F62-348B-4880-BB42-423BA34E0EE4

**Holotype.** UFAC 2793, right part of a rostrum.

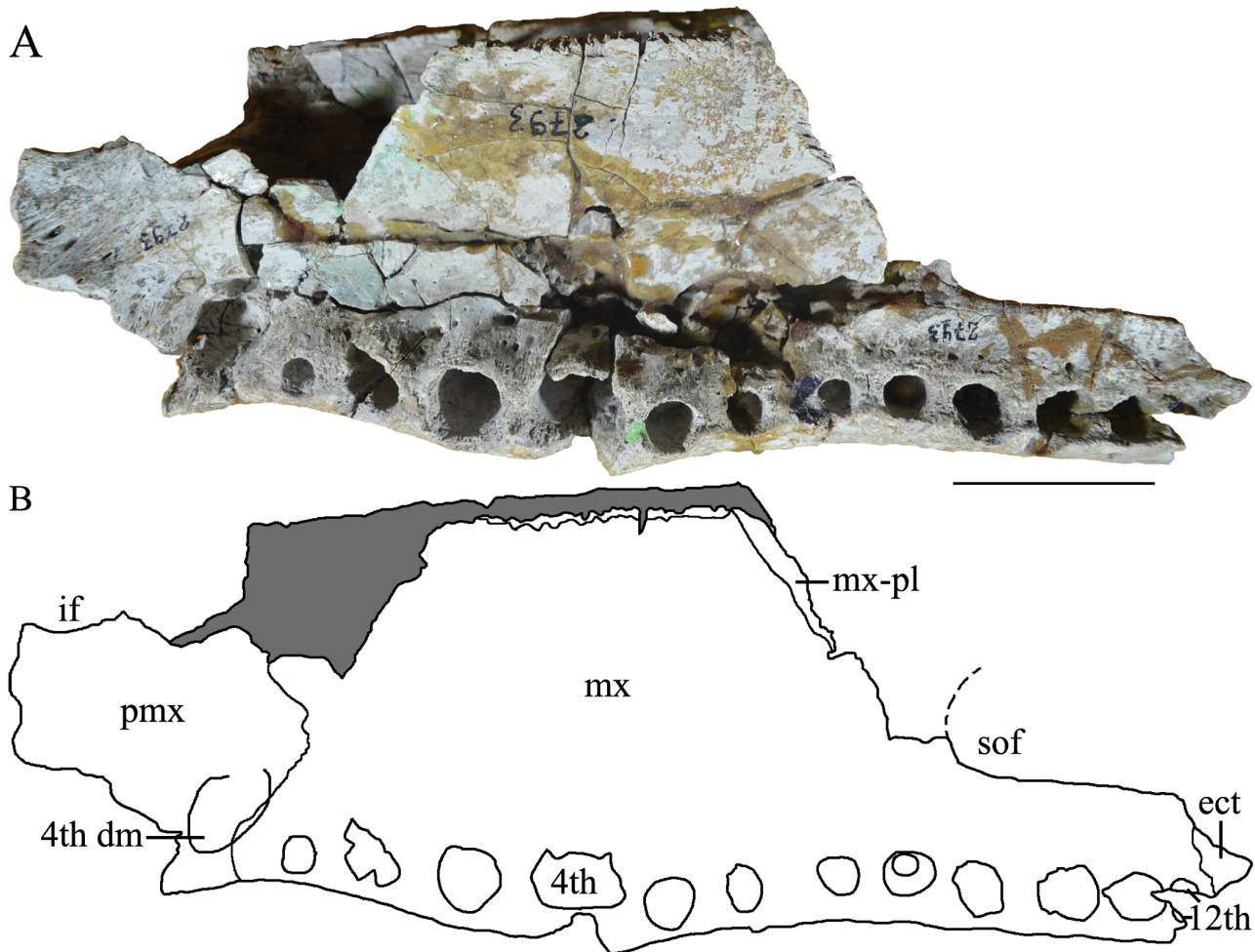
**Etymology.** The specific epithet *latrubessei* is in honor to the Argentinean geomorphologist Dr. Edgardo M. Latrubesse. His geopaleontological contributions were very important to the increase of knowledge about origin and evolution of the Solimões Formation. Dr. Edgardo also provided important scientific contributions for Universidade Federal do Acre through collaborations in partnership with Laboratório de Pesquisas Paleontológicas.

**Diagnosis.** *Melanosuchus latrubessei* possess the following autapomorphies: (1) the contact between maxilla-maxilla is elongated and extends from the space between the second and third alveoli until to the space between the sixth and seventh alveoli; and (2) the rostral ridge 2 is well-developed and well-marked, being anteroposteriorly inclined, and composed exclusively by the maxillary bone.



**FIGURE 2.** *Melanosuchus latrubessei* UFAC 2793 in dorsal view. (A) UFAC 2793 fossil specimen; and (B) Schematic draw. Anatomical abbreviations: **if**, incisive foramen; **EN**, external nares; **J**, jugal; **pmx**, premaxilla; **mx**, maxilla; **n**, nasal; **rd1**, rostral ridge 1; **rd2**, rostral ridge 2. Scale bar = 20mm.





**FIGURE 3.** *Melanosuchus latrubessei* UFAC 2793 in ventral view. (A) UFAC 2793 fossil specimen; and (B) Schematic draw. Anatomical abbreviations: **4<sup>th</sup>**, fourth maxillary alveolus; **4<sup>th</sup> dm**, tooth mark from fourth dentary; **12<sup>th</sup>**, twelfth maxillary alveolus; **ect**, ectopterygoid; **if**, incisive foramen; **pmx**, premaxilla; **mx-pl**, suture between maxillary and palatine; **mx**, maxilla; **sof**, suborbital (palatine) fenestrae. Scale bar = 20mm.

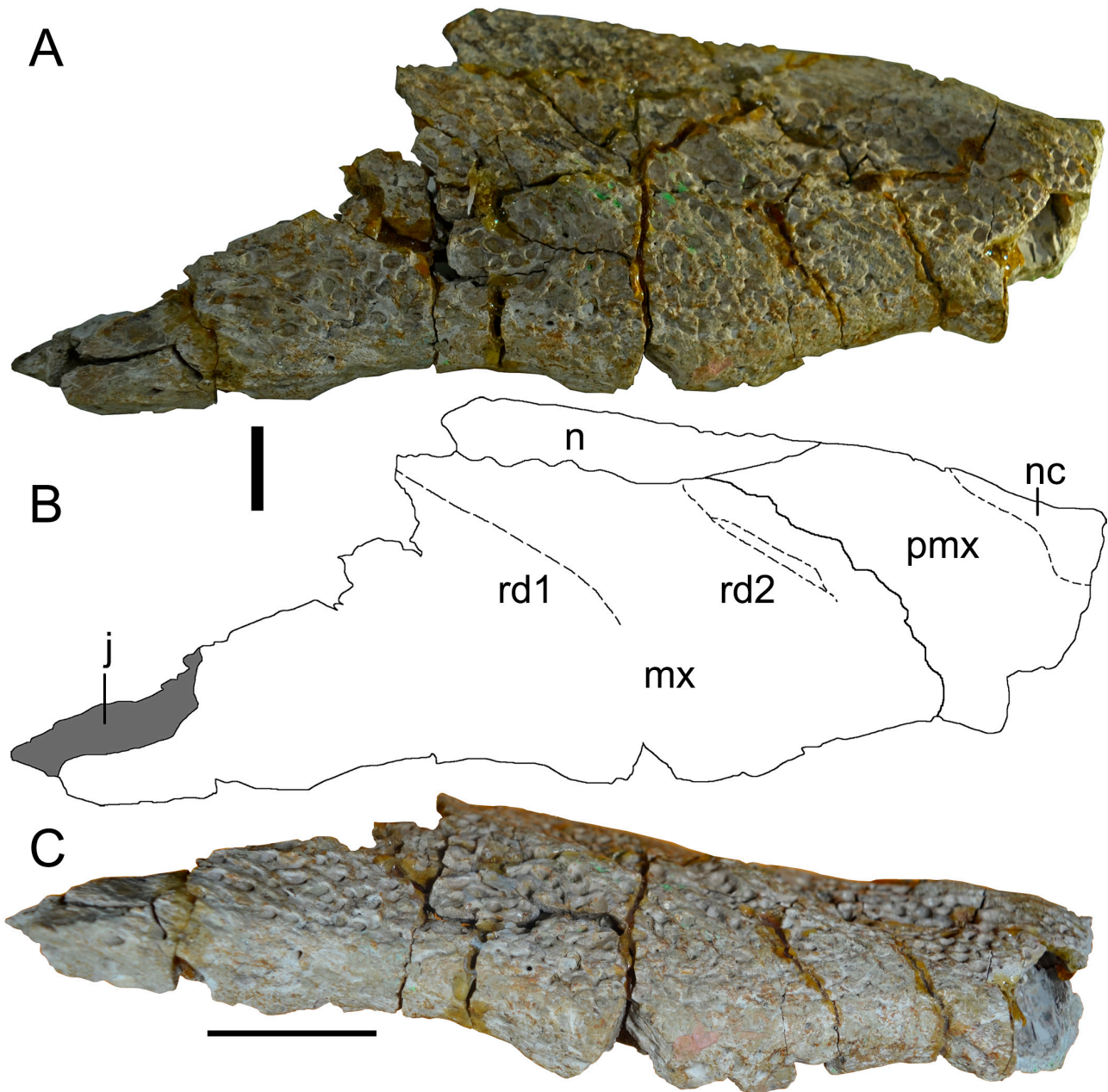
**Occurrence.** The Talismã outcrop is located on the bank of the Purus River, in Southern region of the Amazonas State, Brazil (08°46'37,8"S; 68°54'15,1"W; Figure 1). The outcrop has approximately eight meters of vertical length and the rocks are formed by fine grained silts and clays floodplain sediments, with secondary gypsum and carbonate veins. Presenting his maximum deposition  $10.89 \pm 0.13$  Ma, being at least Tortonian in age (Bissaro-Júnior *et al.* 2019).

**Description.** The skull fragment has a maximum length of 287 mm and maximum width of 87.7 mm (measured at the level of third maxillary alveolus). The holotype of *M. latrubessei*, UFAC 2793, consists on the right half of the rostrum, with only the posterior portion of the premaxilla preserved, almost complete maxilla and the nasal bone lacking the most posterior region (Figure 2, 3 and 4). A small fragment of the right ectopterygoid is also preserved and articulated with the posterior portion of the maxilla (Figure 3). The premaxilla lacks most of the lateral and anterior region; therefore, no alveoli is preserved. In dorsal view, the premaxilla, preserves the right lateral and posterior portions of the external nares (Figure 2) and, in ventral view, preserves only the right lateral margin of incisive foramen (Figure 3). The maxilla has preserved the joint surface with the jugal, which can be seen in the dorsal and lateral views (Figure 2 and 4). In ventral view, the maxilla presents, in its posterior middle corner, the articular surface of the anterior process of the palatine and on the lateral margin, twelve alveoli (Figure 4). No diagenetic torsions or modifications, beside those of the broken portions, are observed.

*M. latrubessei* UFAC 2793 presents a well-marked bone ornamentation uniformly distributed along the entire dorsal surface of the rostrum, with exception of the region around the external nares (Figure 2 and 4). The ornamentation consists of irregular but usually round and well-marked pits, with small variations in size. The external nares

have only the posterior margin and the posterior lateral margin preserved (Figure 2). The posterior margin, although not complete, appears to form an almost straight line, with a shallow convexity at the transition to the lateral margins. The lateral margin opens laterally, with the anterior portion more lateralized than the posterior, this inclination makes the anterior margin of the external nares wider than the posterior one (Figure 2).

Only the right lateral middle portion of the incisive foramen is preserved, this portion represents a shallow concavity that is in the posterior portion of the premaxilla (Figure 3). However, in the absence of premaxillary alveoli and the fragmentary condition of the structure, the exact location and shape of the incisive foramen can only be tentatively inferred. This shallow concavity seems to be related to an anteroposteriorly long incisive foramen, which probably extends from the last and penultimate premaxillary alveoli to, at least, the third premaxillary alveoli (considering five premaxillary alveoli, found in *Crocodylia*—Brochu 1999, 2011, 2013). However, the shape of incisive foramen as a whole cannot be inferred.

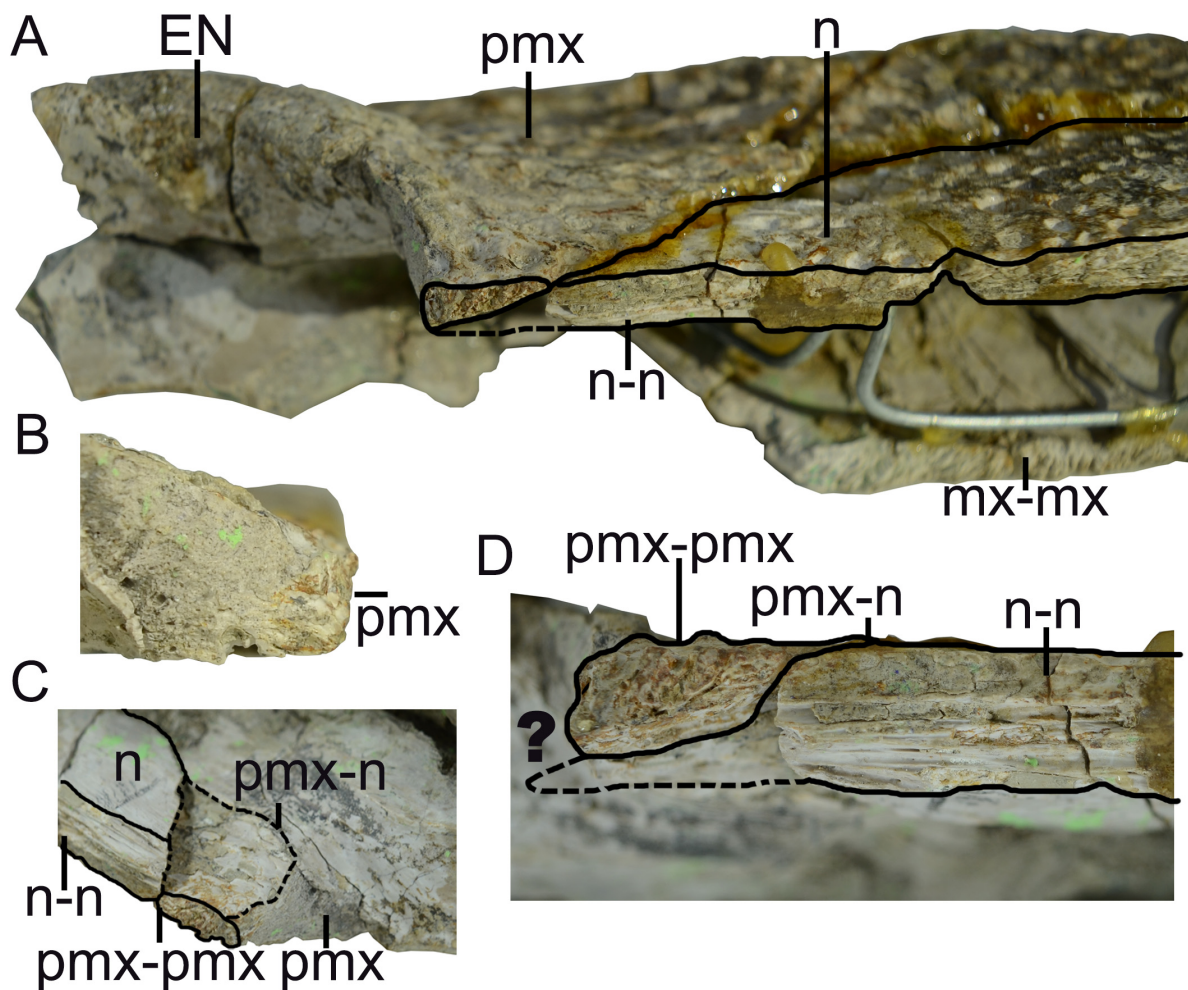


**FIGURE 4.** *Melanosuchus latrubessei* UFAC 2793. (A) UFAC 2793 fossil specimen in laterodorsal view; (B) Schematic draw in laterodorsal view; and (C) fossil specimen in lateral view. Anatomical abbreviations: **J**, jugal; **pmx**, premaxilla; **mx**, maxilla; **n**, nasal; **nc**, narial crest; **rd1**, rostral ridge 1; **rd2**, rostral ridge 2. Scale bar, A and B = 20mm; C = 50mm.



The right suborbital fenestra is partially preserved, and only the portions that contribute to the maxilla are present, with the anterior portion of the lateral margin and the lateral portion of the anterior margin (Figure 3). The preserved anterior margin is a shallow concavity and the lateral margin is straight and slightly inclined mediolaterally, with the anterior portion more medial than the posterior one (Figure 3). The maxillary margin of the suborbital fenestra is straight, without any projection in the fenestra; moreover, the anterior margin of suborbital fenestra reaches the space between the ninth and the eighth alveoli (Figure 3).

The premaxilla, in dorsal view, has a posterior wedge-shaped process that extends until the position of the third maxillary alveolus. This posterior process has the apex aligned with the suture between the maxillary-nasal, being the lateral portion of the premaxilla posterior process sutured with the maxilla, in the most anterior part, and medially with the nasal bone (Figure 2 and 4). The premaxilla has a continuous crest delimiting the lateral and posterior limits of the external nares, which is here referred as narial crest (Figure 2 and 4). It is important to note that, in dorsal view, the right premaxilla sutures with the left premaxilla, at least dorsally, with this contact being located immediately posterior to the margin of the external nares (Figure 2). The premaxilla-premaxilla contact in dorsal view can be better evidenced in a sagittal cut, where the medial surface of the right premaxilla and right nasal can be observed (Figure 5). The posterior margin of the external nares, composed entirely by the premaxilla, is preserved and does not have sutures with the nasal bones (Figure 5 a, b).



**FIGURE 5.** *Melanosuchus latrubessei* UFAC 2793 in detail of the premaxillary-nasal anterior region. (A) Anterodorsomedial view of the right elements, via sagittal cut, elucidating the limits between premaxilla and nasal; (B) Anterior view of premaxilla, within the external nares, elucidating the absence of premaxilla-nasal suture at this view; (C) Medioventral view demonstrating the overlap suture of premaxilla over nasal; and, (D) Medial view of right elements, via sagittal cut, demarked limits between premaxilla and nasals demonstrating the only possible way to nasal reach the external nares. Full line indicates visible sutures while dashed lines indicated inferred bone limits. Anatomical abbreviations: **EN**, external nares; **pmx-n**, suture between premaxilla and nasal; **pmx-pmx**, suture between premaxillae; **pmx**, premaxilla; **mx-mx**, suture between maxillae; **n-n**, suture between nasals; **n**, nasal. Out of scale.



The anterior portion of the nasal bone is broken, immediately above the anterior portion of the premaxilla. However the premaxilla is complete, indicating an overlapping suture (i.e. at least at this anterior portion the premaxilla lies over the nasal) (Figure 5 a, d). This relation between premaxilla and nasal can be better understood due to the break of the nasal in ventral view, which evidences a contact between those bones and not a fusion demarcating a suture (Figure 5 c). Moreover, the medial surface of the premaxilla is rugose as expected to a premaxilla-premaxilla contact, while the nasal bones present a horizontal and parallel lines, as expected in nasal-nasal contact (Figure 5 d). The nasal bone is broad in the lateromedial direction, with its anterior wedge-shaped projection. The premaxillary-maxillary suture contacts the lateral limit of the nasal at the point where the wedge-shaped process begins (Figure 2).

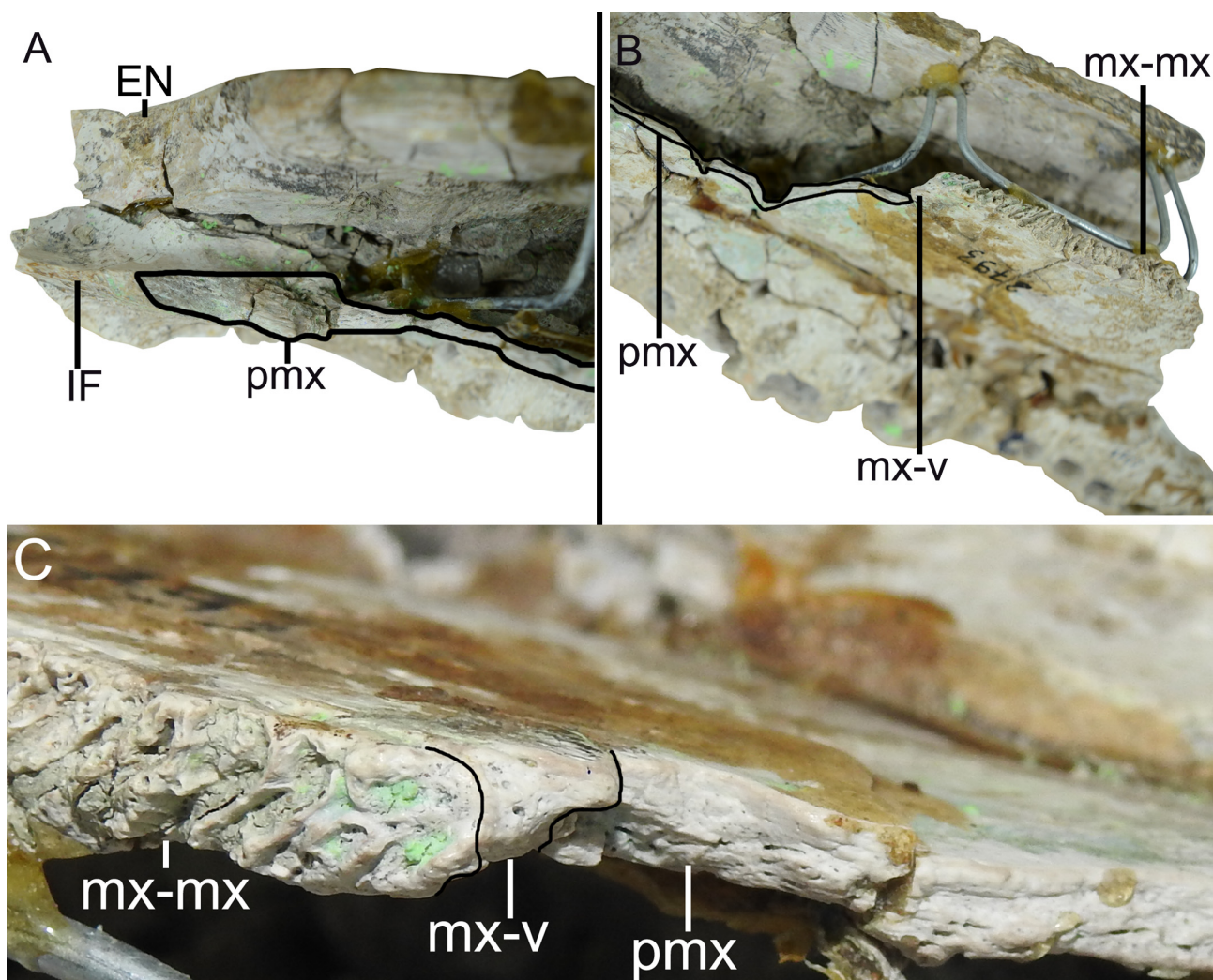
The maxilla, in dorsal view, contacts anteriorly with the premaxilla and nasal, while having exclusive medial contact with the nasal bone (Figure 2 and 4). There are a total of twelve maxillary alveoli. The longitudinal measurements of each alveolus, from the anterior most to the posterior most are, respectively (in mm): 6.88; 11.33; 14.75; 17.95; 9.58; 7.65; 7.29; 9.46; 11.32; 11.36; 10.9; and 8.19. The eighth alveolus has a preserved tooth, which did not have a complete dental eruption *in vivo*; therefore, the non-exposure of this tooth prevents a detailed description of its morphology. However, the apex of the tooth is visible and represents a convex structure.

The lateral border of maxilla, in dorsal and ventral views, has the anterior (position anteriorly to the first maxillary alveolus) and posterior (position of the eleventh and twelfth maxillary alveoli) portions projecting laterally. At the level of the fourth alveolus, in both dorsal and ventral views, there is a well-developed convexity (Figure 2 and 4). In lateral view, the ventral margin of the maxilla has a well-marked concavity anteriorly to the convexity at the level of fourth maxillary alveolus, and posterior to this convexity there is another shallow concavity (Figure 4). In the posterior region of the maxilla, there is a surface corresponding to the contact between maxilla-jugal, where the jugal bone overlies the maxilla (Figure 2 and 4). However, the jugal is not preserved.

The maxilla also has two well-developed rostral ridges (Figure 2 and 4). The first (rostral ridge 1) is associated with the high development of the *canthi rostralii*; thus, although the interorbital region is not preserved, the presence of a well-developed *canthi rostralii* is proposed. Therefore, this difference in saturation surface reinforces the idea of a premaxilla-premaxilla contact exposed in dorsal view. However, as the nasal is not entirely preserved, we cannot rule out the possibility of nasal bones with a continuous contribution with the anterior process within the external nares, passing below the premaxilla-premaxilla contact (Figure 5 d). In ventral view, the premaxilla-maxilla suture passes within the tooth occlusal pit. From the fourth dentary, and posteriorly to this excavation the suture has a small posterior wedge-shaped process that extend to the posterior end of the first maxillary alveoli (Figure 3). The other rostral ridge (rostral ridge 2) is entirely located within the maxilla next to the premaxilla-maxilla suture, in dorsal view (Figure 2 and 4), and represents a dorsoventrally inclined bone intumescence, with the anterior portion ventral to the posterior (Figure 4). In ventral view, the maxilla-maxilla suture extends straight from the third to the sixth alveolus (Figure 3). Prior to the maxilla-maxilla suture, there is a smooth maxillary portion that opens slightly laterally and is here interpreted as the contact surface with the vomer. At the posterior limit of the maxilla, immediately behind the intermaxillary suture, there is the sutural region of the palatine, which is evidenced by a surface with thin crests. Thus, the palatine extends anteriorly to the level of the sixth alveoli (Figure 3).

At the posterior limit of the maxilla in ventral view, immediately posterior to the tooth row, there is the maxilla-ectopterygoid contact, with a small portion of the anterior region of the ectopterygoid being preserved (Figure 3). The ectopterygoid does not form the medial margin of any maxillary alveolus and the anterior process of this structure does not exceed the twelfth maxillary alveolus (Figure 3). The lateral portion of the maxilla to the suborbital fenestra is wide, being at least twice the width of the tenth alveolus (Figure 3).

Despite the fact that the vomer is not preserved and the region between the maxilla and premaxilla is severely damaged, there are some clear evidences in both the premaxilla and the maxilla of the presence of the vomer, which will be presented below. The first evidence is the presence of the aforementioned smooth anterior surface to the end of the maxilla-maxilla suture, which opens laterally and corresponds to the articular surface between the maxilla and the vomer (Figure 2 and Figure 6 b, c). The second evidence can be seen in medial view, due to the sagittal cut where the ventral portion of premaxilla has an intumescent region, which is broken but clearly detectable, with this structure being correspondent to the posterior portion of the premaxilla that contacts the anterior limit of the vomer (Figure 6 a). Additionally, it is important to note that the broken pattern observed in the transition zone between premaxilla and maxilla can be expected for a specimen with an exposed vomer, as the presence of the vomer creates a fragilized zone in this portion of the rostrum.



**FIGURE 6.** *Melanosuchus latrubessei* UFAC 2793 in details of the maxillary and premaxillary limits of the ventral portion in medial view. (A) Elucidating the preserved anterior limit of premaxilla; (B) The anterior limit of maxilla-maxilla suture and the posterior broken region of premaxilla; and (C) Zoom in the limit maxilla-maxilla suture elucidating an anterior smooth surface that is here inferred as the posterior limit for maxillary-vomer contact. Dark lines delimit the bone limits and sutures. Anatomical abbreviations: **if**, incisive foramen; **EN**, external nares; **pmx**, premaxilla; **mx-mx**, suture between maxillae; **mx-v**, suture between maxillary and vomer. Out of scale.

**Comparisons.** *Melanosuchus latrubessei* shares with *Melanosuchus niger* the presence of a vomer that is exposed and located between the premaxilla-maxilla suture, as well as the well-developed rostral ridges, mainly the second and most anterior one. Other similarities worth mentioning here are: (1) the external nares with a keyhole-shaped or circular format; (2) the premaxilla which has a right and left posterior processes, in ventral view, that does not surpass posteriorly the first maxillary alveoli; (3) the premaxilla-premaxilla contact at the dorsal surface immediately behind the posterior margin of the external nares, which represents an intraspecific variation within *M. niger*; that can have the nasal bones reaching the external nares and being exposed dorsally inhibiting the premaxilla-premaxilla contact at this region; (4) the palatine, which projects well anterior to the end of the suborbital fenestrae and has an expanded anterior end; and, (5) the anterior margin of the suborbital fenestrae reaches the space between the eighth and ninth maxillary alveoli (differing from MCNC 243 specimen - former *M. fisheri*, which reaches the space between ninth and tenth alveoli).

The vomer exposure on the palate between premaxilla and maxilla is a characteristic of *M. niger* (e.g. Mook 1921; Medem 1963; Iordansky 1973; Brochu 1999; Bona *et al.* 2017b), and this feature was used as diagnosis to assign the fossil specimens to this genus (e.g. Medina 1976). However, the bone has never been properly described, even in detailed works on *M. niger* (e.g. Mook 1921; Medem 1963; Iordansky 1973; Medina 1976; Brochu 1999;

Vieira *et al.* 2016; Bona *et al.* 2017b). In this work, we recognize the vomer as a hollow paired bone, located between the premaxilla and maxilla, in the medial and anterior region of the rostrum, with the paired bones being attached only by a contact, and not by a real suture. This can be evidenced by the thin projections from the maxillae, which overlap ventrally and dorsally the posterior and lateral limits of the vomer (Figure 7). The anterior portion of the vomer attaches, without suturing, to the posterior premaxillary intumescence (Figure 7).

The hollowness of the vomer, together with its weak contact towards the premaxilla and maxilla, make this bone and the surrounding area more fragile when the animal is dead; therefore, it is common the loss of the vomer with the break and/or disarticulation of associated bones, as observed in *M. latrubessei* (Figure 3; this is also evidenced in the studied *M. niger*, see Table 1). However, we reinforce that the existence of the vomer in *M. latrubessei* is supported by two features: (1) the anterior end of maxilla-maxilla suture at the palate culminates in a smooth maxillary surface that opens laterally (Figure 6 b, c); and, (2) the premaxilla, in medial view from a sagittal cut, has at the posterior portion of the ventral surface an intumescence that was broken in the *M. latrubessei* specimen, but the characteristic brands remained (Figure 6 a). The condition observed in *M. latrubessei* diverges from that seen in *Caiman* genus, which has the vomer restricted to the narial passage and located posteriorly, aligned with the prefrontals (e.g. Bona & Desojo 2011). It also diverges from *Paleosuchus palpebrosus* (Cuvier 1807) and the *Caiman* species by exhibiting premaxillae that are thicker and more robust than the maxillae (Figure 7 c, d). For vomer condition in *Alligator* see Rieppel (1993).

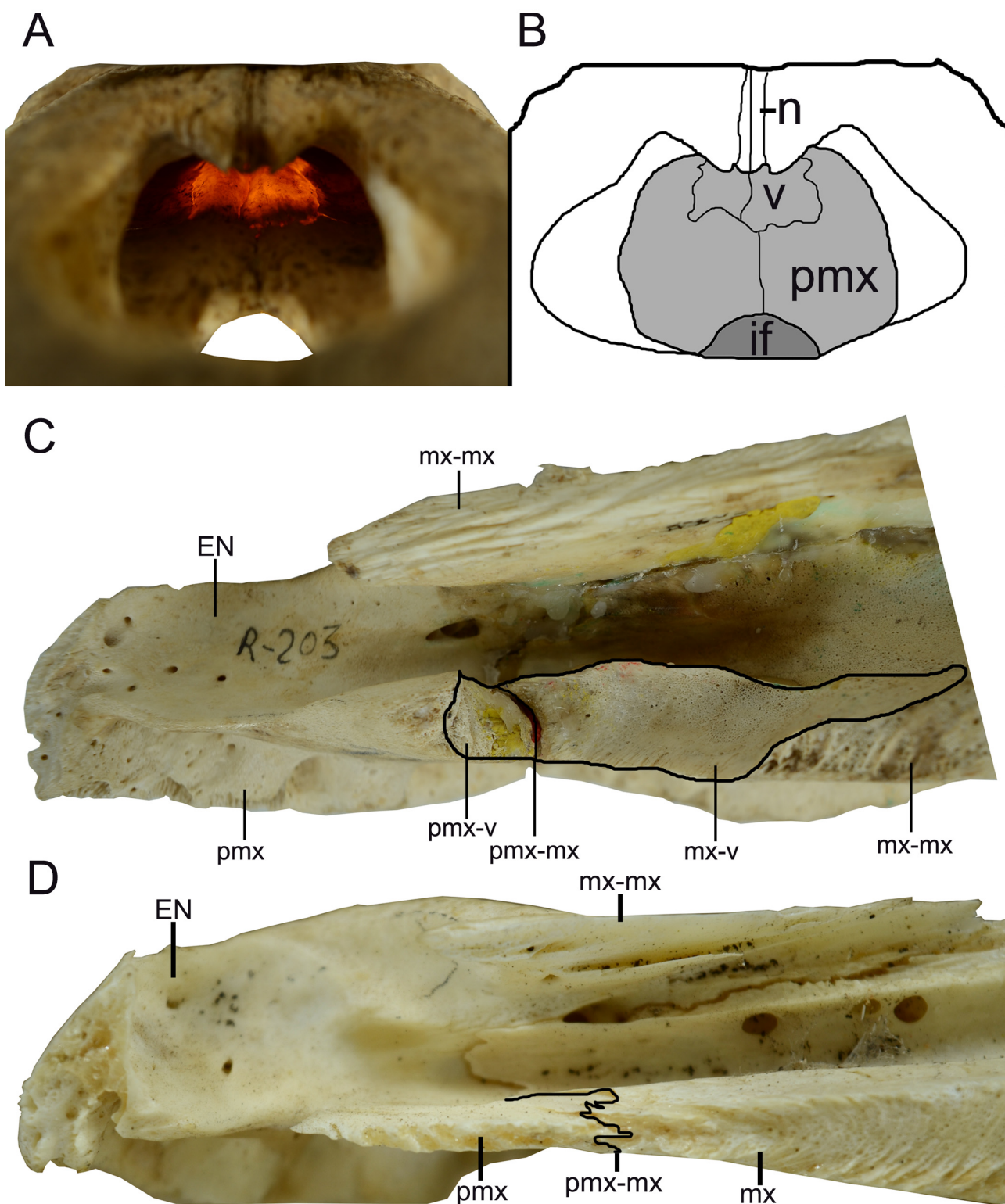
Despite the aforementioned similarities shared between *M. latrubessei* and *M. niger*, they also present several differences that should be highlighted, such as: (1) *M. latrubessei* presents twelve maxillary alveoli, while *M. niger* has thirteen (including MCNC 243); (2) the narial crest in *M. latrubessei* is restricted to the border of the external nares and is isolated from the rostral ridges (Figure 4), while in *M. niger* the narial crest at the posterior corner of external nares has a posterior projection bordering the premaxilla-nasal suture, being associated with the rostral ridges (Figure 8); (3) the maxilla-maxilla contact, in the palatal surface, of *M. latrubessei* extends from the third to the sixth maxillary alveoli, while in *M. niger* (including MCNC 243), despite the intraspecific variability and asymmetrical development in some pathological specimens, this contact keeps restricted between the second and the fourth maxillary alveoli, or even less (e.g.; in some specimens, this contact extends from the third to the fifth maxillary alveoli); (4) the anterior process of the ectopterygoid in *M. latrubessei* is inclined medially, stretching for one maxillary alveolus (the twelfth), while for *M. niger* (including MCNC 243), the anterior process is straighter and extends by two or three alveoli (reaching the twelfth/thirteenth maxillary alveoli); and, (5) despite the fact that *M. latrubessei* and *M. niger* exhibit two rostral ridges in the rostrum, it is important to mention that in *M. latrubessei* the rostral ridge 2 is developed and well-marked, being anteroposteriorly inclined, and completely composed by the maxilla without contacting the rostral ridge 1, while in *M. niger* (including MCNC 243), the rostral ridge 2 is located over or very close to the premaxilla-maxilla suture, extending from the dorsal surface until reaching the ventral margin of the aforementioned suture, being this ridge connected with the rostral ridge 2 (Figure 8).

All studied specimens (see Table 1) present a similar pattern of ornamentation, with irregular, but generally round and well-marked pits along the entirely dorsal surface of the rostrum. However, only in *M. latrubessei* this bone ornamentation does not reach the margins of the external nares (Figure 2). Though fragmented, the preserved portion of the external nares in *M. latrubessei* enables to infer a circular or keyhole-shaped format, as stated earlier (Figure 2); this condition (character83[0]) is shared with all other studied specimens (see Table 1).

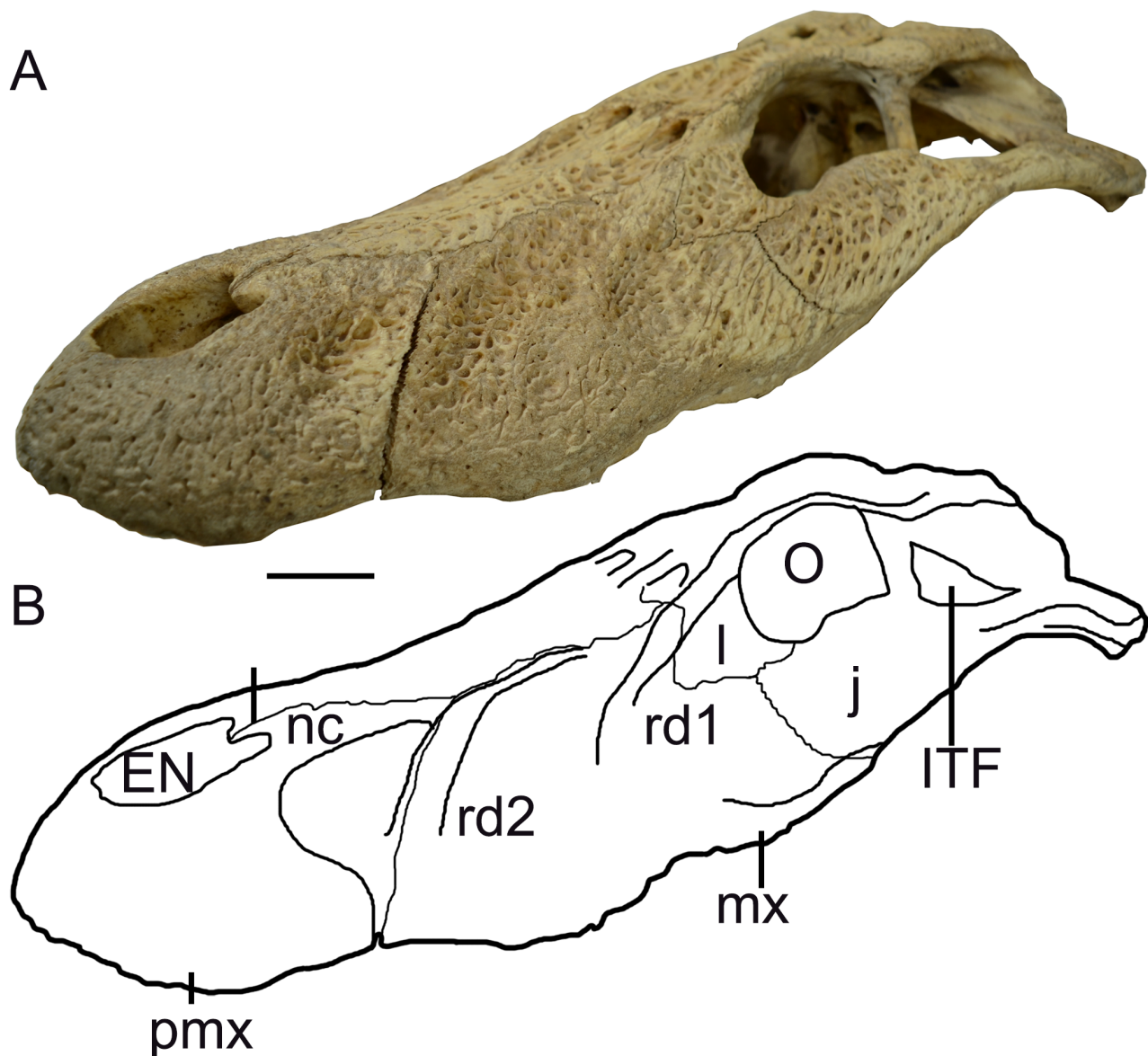
The incisive foramen is only partially preserved in *M. latrubessei* (Figure 3), but since the lateral margin is well-preserved, based on the maximum curvature, it is possible to stipulate the anterior and posterior limits of the incisive foramen. In this scenario, the incisive foramen occupies less than half of the premaxillae maximum length (88[0]). The same condition is seen in other studied specimens, with exception of *Caiman brevirostris* and *Caiman wannlangstoni* Salas-Gismondi *et al.* 2015, which do not have this portion preserved. Regarding the location of the incisive foramen, in relation to the premaxillary toothrow, it is inconclusive to assert that in *M. latrubessei* this foramen protrudes between the first premaxillary alveoli, as can be seen in the fossil specimen UCMP 39978 and in *M. niger*, as well as in *Caiman* species.

The anterior limit of the suborbital fenestra in *M. latrubessei* is located between the eighth and ninth maxillary alveoli, similar to observed in *Caiman crocodilus* (Linnaeus 1758), *Caiman latirostris* (Daudin 1802), *Caiman yacare* (Daudin 1802), *M. niger* and UCMP 39978. As it was already mentioned, the suborbital fenestra in MCNC 243 (former *M. fisheri*) reaches the space between the ninth and the tenth alveoli. The lateral margin of the suborbital fenestra comprised by the maxillary process is linear in all studied specimens (111[0]; Table 1), with exception of *Caiman brevirostris* and *Caiman gasparinae* Bona & Carabajal 2013, which do not preserve this portion.





**FIGURE 7.** The vomer anatomy of *Melanosuchus niger* specimens (UFAC R-136 and UFAC R-203) in comparison with *Paleosuchus palpebrosus* specimen (UFAC R-215). (A) Anterodorsal view of the inside of external nares, in red, the articulated vomer in *Melanosuchus niger* (UFAC R-136); (B) Schematic draw of figure A; (C) Medial view of right rostrum of *Melanosuchus niger* (UFAC R-203) highlighting the contacts of vomer with premaxilla and maxilla after the bone removal; and (D) *Paleosuchus palpebrosus* specimen (UFAC R-215) illustrating an example where the vomer is fused with other bones. Dark lines mark bone limits and sutures. Anatomical abbreviations: **if**, incisive foramen; **EN**, external nares; **pmx-mx**, suture between premaxillary and maxillary; **pmx-v**, suture between premaxilla and vomer; **pmx**, premaxilla; **mx-mx**, suture between maxillae; **mx-v**, suture between maxillary and vomer; **mx**, maxilla; **n**, nasal; **v**, vomer. Out of scale.



**FIGURE 8.** *Melanosuchus niger* UFAC R-203 in anterolateral view. (A) Original specimen; (B) Schematic draw elucidating the presence and positioning of the rostral ridges. Anatomical abbreviations: l, lacrimal; EN, external nares; ITF, infratemporal fenestra; J, jugal; pmx, premaxilla; mx, maxilla; n, nasal; nc, narial crest; O, orbit; rd1, rostral ridge 1; rd2, rostral ridge 2. Scale bar = 20mm.

The premaxilla exhibits, in dorsal view, two symmetrical posterior wedge-shaped processes that extend through three maxillary alveoli in *Caiman brevirostris*, *C. crocodilus*, *C. latirostris*, *C. yacare*, *M. niger* (including MCNC 243), *M. latrubessei* and UCMP 39978, in contrast to *C. gasparinae*, in which this projection does not surpass posteriorly any of that maxillary alveoli, being almost lateromedially straight. In ventral view, all specimens studied have the posterior premaxillary process restricted to the level of the first maxillary alveoli. Both conditions are unknown in *C. wannlangstoni*.

The nasal bones contact the posterior border of the external nares, but do not bisect it (82[1]), as seen in *Caiman brevirostris*, *C. crocodilus*, *C. latirostris*, *C. wannlangstoni*, *C. yacare*, and *M. niger* (at least some specimens, including MCNC 243), contrasting with the observed in *C. gasparinae* and *M. latrubessei*, in which the nasals are posteriorly retracted (at least externally) from the external nares, with the premaxillae contacting laterally in the medial line of the dorsal surface (82[2]). This condition is unknown in the UCMP 39978 specimen.

All studied specimens (Table 1), with exception of *Caiman wannlangstoni* (that does not have this portion preserved), have the fourth dentary tooth leaving an occlusion pit in the format of a deep excavation, located between

the last premaxillary and first maxillary alveoli, in the contact between these two bones. A similar condition is observed in *M. latrubessei* (Figure 3).

The anterior extension of the wedge-shaped ectopterygoid process lateral to the toothrow is quite variable in Caimaninae species. In *M. latrubessei* this process is inclined medially and extends for only one maxillary alveolus, while in *M. niger* (unknown in MCNC 243), the process is straighter and extends along the two or three most posterior maxillary alveoli. There are some species with an anterior process of the ectopterygoid elongated, that extends for three maxillary alveoli, such as *Caiman latirostris*, *C. wannlangstoni* and UCMP 39978, or even for four maxillary alveoli, such as in *C. crocodylus* and *C. yacare*. This condition is unknown in *C. brevirostris* and *C. gasparinae*.

The species that do not exhibit an exposed vomer, such as *Caiman crocodylus*, *C. latirostris*, *C. yacare* and the specimen UCMP 39978, have the maxilla-maxilla contact, in ventral view, extending for six maxillary alveoli. The only exception is *C. brevirostris*, where this contact extends for four maxillary alveoli. Among the species with an exposed vomer, *M. niger* (including MCNC 243) present the contact that extends for three maxillary alveoli while in *M. latrubessei* the maxilla-maxilla medial contact extends for four maxillary alveoli (Figure 3). This condition is unknown in *C. gasparinae* and *C. wannlangstoni*.

Considering mature specimens, the *canthi rostralii* is absent or very modest (96[0]) in *Caiman crocodylus*, *C. gasparinae* and *C. yacare*, contrasting with the very prominent condition (96[1]) observed in *C. brevirostris*, *C. latirostris*, *C. wannlangstoni*, *M. niger*, *M. latrubessei* and UCMP 39978 specimen. Associated to the well-developed *canthi rostralii*, there is the rostral ridge 1. The development of the rostral ridge 1 indicates prominent *canthi rostralii* in *M. latrubessei*. The rostral ridge 2 is developed at maturity only in *M. niger* and *M. latrubessei*, being not well-developed in the remaining studied species (see Table 1).

**Remarks.** Some comparisons use the relative position of the structure in reference to the maxillary alveoli. The number of maxillary alveoli in Caimaninae seems to have very few to null intraspecific variation (Bona *et al.* 2017b), serving as a basis for other structure comparisons. However, as *M. latrubessei* and *M. niger* have different number of alveoli in the maxilla, those comparisons could be equivocated. This alveoli variation between *Melanosuchus* species could be result of two processes equally possible: (1) either the thirteenth alveoli was reduced and disappeared in *M. latrubessei*; or (2) it emerged and was fixed among *M. niger* specimens. Also, all references were based on the middle to anterior alveoli that seems to have a homologue correspondence between these species, based on their morphology. Therefore, this different alveolar number in maxilla cannot be considered a problem with the references provided by the other structures. The only exception for these morphological references is the anterior extension of the ectopterygoid, where in *M. niger* extends for two maxillary alveoli, while in *M. latrubessei*, it extends for one and this variation seems to be biologically dependent with the different alveolar count that is varying in the posterior region of maxilla. Therefore, it is not possible to assure that this difference in alveolar count is the result of a well-extended anterior process of the ectopterygoid in *M. niger* or due to the absence of an alveolus in *M. latrubessei*.

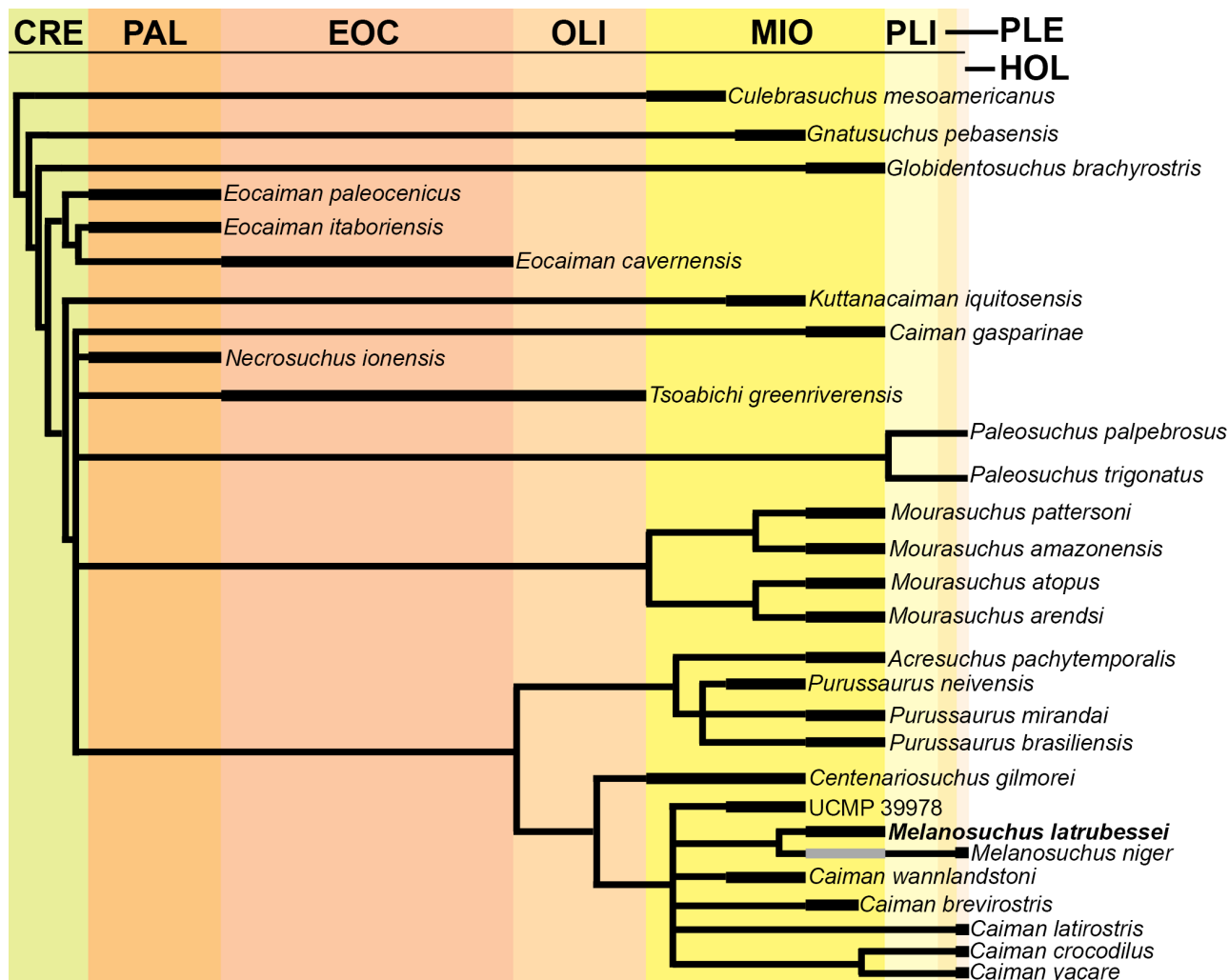
The rostral ridge 2 varies in size and robustness among the studied specimens of *M. niger* (including MCNC 243), and this variation is strongly correlated to the maturity of the specimens, with the ridge being more robust and developed in large and adult animals (Figure 8). However, in none of the observed skulls the rostral ridge 2 presents significant variation in position, being located over or very close to the premaxilla-maxilla suture in all specimens (e.g. Figure 8). Additionally, the rostral ridge 2 in *M. latrubessei* is completely isolated from the rostral ridge 1, which is opposed to the feature observed in all studied *M. niger* (Table 1). Therefore, the present work considers that the rostral ridges 2 in *M. latrubessei* and *M. niger* are homologous structures, even located in different portions of the rostrum. Such differences in position and morphology are related to interspecific variation.

The general prismatic morphology of the vomer among *Melanosuchus* specimens (e.g. Brochu 1999; Vieira *et al.* 2016) is quite variable, going from a more circular to a more angular prismatic shape. This morphological variation is reflected in the morphology of the premaxilla and maxilla, but in all studied specimens the pattern described here (Figure 7) was observed. In *Melanosuchus*, the morphology and position of the vomer has some similarities with Squamata species (e.g. Jollie 1960; Avery & Tanner 1971; Gauthier *et al.* 2012), however, there is no available discussion or literature about the *Melanosuchus* vomer. Thus, further studies are necessary for a better understanding regarding the embryology, ontogeny and function of the structure.



## Phylogenetic inference

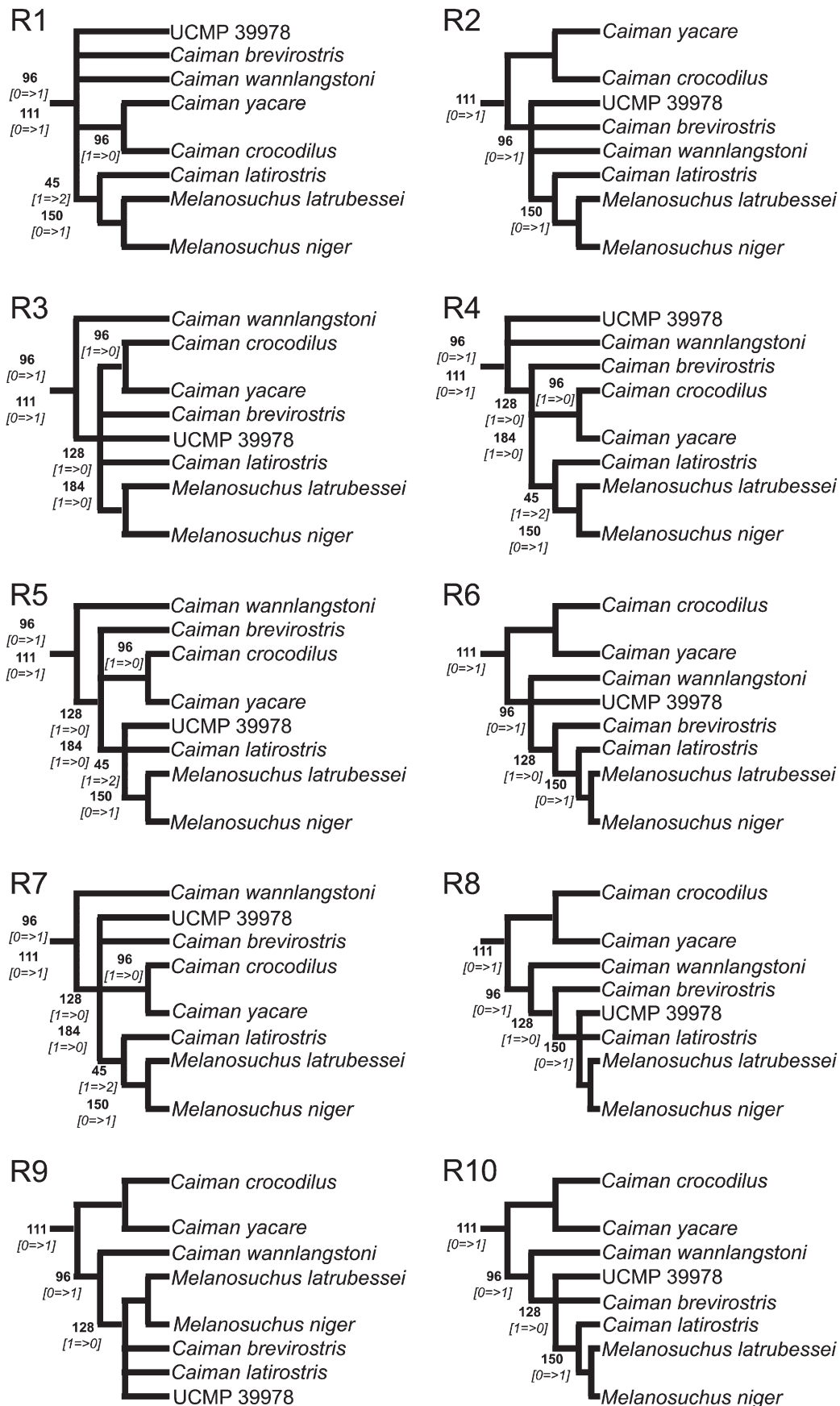
The phylogenetic inference resulted in a 16,800 MLT with 641 steps (CI: 0.382; RI: 0.807), and the complete strict consensus cladogram is available in Figure S1. A simplified and temporally calibrated version of the strict consensus cladogram, focused in Caimaninae clade, is presented in Figure 9. The new species was recovered as sister species of *Melanosuchus niger*, justifying our proposition as belonging to *Melanosuchus* genus. The genus *Melanosuchus*, in turn, was nested within a polytomy known as Jacarea (*sensu* Brochu 1999) (Figure 9).



**FIGURE 9.** Calibrated consensus cladogram from 16,800 MLT with 641 steps (CI: 0.382; RI: 0.807) restricted to Caimaninae. The thin lines indicate the inferred relationships. Dark large lines indicate the known temporal occurrence of the species. Gray large line indicate the known temporal occurrence of *Melanosuchus* cf. *M. niger* or *Melanosuchus* indet.

The Caimaninae clade, in all trees, accounts for the following characteristics: (1) the largest maxillary alveolus is the third (93[0]), fixed from an ancestral with the fourth being the largest maxillary alveolus (93[1]); and, (2) the supraoccipital is exposed on dorsal skull table isolating the parietal from the posterior edge of the table (159[3]), fixed from an ancestral with a small exposure of the supraoccipital (159[0]).

The polytomy including *Caiman gasparinae*, *Necrosuchus ionensis* Simpson 1937, *Tsoabichi greenriverensis* Brochu 2010, *Paleosuchus*, *Mourasuchus*, *Acresuchus pachytemporalis*, *Purussaurus*, *Centenariosuchus gilmorei* Hastings *et al.* 2013, UCMP 39978, remaining *Caiman* species and *Melanosuchus* is supported in all trees by the following characteristics: (1) dentary symphysis extends to fourth or fifth alveolus (49[0]), originated and fixed from an ancestral in which the dentary symphysis extends to sixth to eighth alveolus (49[1]); (2) maxilla has linear medial margin adjacent to suborbital fenestra (111[0]), fixed from an ancestral with a broad shelf extending into fenestra, making lateral margin concave (111[1]); and, (3) dorsal edges of orbits upturned (136[1]), feature derived from an ancestral with the margin of orbit flush with skull surface (136[0]).



**FIGURE 10.** Jacarea relationships from MLT's that generated the polytomy in the strict consensus. Bold numbers refer to the number of the character in character list and the italic numbers demonstrated the condition of the character in both ancestral and descendent species.

The clade that includes *Centenariosuchus* + *Jacarea* (excluding *Caiman gasparinae*) accounts in all trees for the incisive foramen projected between the first premaxillary teeth (89[2]), feature originated and fixed from an ancestral population where the incisive foramen is completely situated far from the premaxillary tooth row, at the level of the second or third alveolus (89[0]).

The clade *Jacarea* is a polytomy including UCMP 39978, *Caiman wannlangstoni*, *C. brevirostris*, *C. latirostris*, *C. crocodilus*, *C. yacare*, *M. niger* and *M. latrubessei*. This clade accounts for the presence of a broad shelf extending into fenestra, making lateral margin concave (111[1]), originated and fixed in a population with maxilla having a linear medial margin adjacent to suborbital fenestra (111[0]). In some trees, this clade accounts for the origin and fixation of very prominent *canthi rostralii* at maturity (96[1]), originated from an ancestral population with *canthi rostralii* absent or very modest (96[0]).

The genus *Melanosuchus* was supported in all trees by vomer exposed on palate at premaxilla–maxilla suture (99[1]), feature derived from an ancestral population with the vomer entirely obscured by premaxilla and maxilla (99[0]).

The *Jacarea* polytomy in the strict consensus was the result of ten different combinations of those species within the clade (Figure 10). Here we identify those different topologies assigning the character evolution for each respective topology. A generalized polytomy was recovered in R1 (Figure 10) with only two groups established: (*Caiman yacare* + *C. crocodilus*) and (*C. latirostris* (*M. latrubessei* + *M. niger*)). A polytomy with UCMP 39978, *C. wannlangstoni* and the remaining species is represented in R4 (Figure 10). The topologies where *C. wannlangstoni* diverges first from the rest were R3, R5 and R7 (Figure 10). The most common group to be the first to diverge among the recovered topologies was (*C. yacare* + *C. crocodilus*) in R2, R6, R8, R9 and R10 (Figure 10).

As it was already mentioned, the presence of a broad shelf extending into the suborbital fenestra, making the lateral margin concave (111[1]) was explained by *Jacarea* in all recovered trees. However, in the trees where (*Caiman yacare* + *C. crocodilus*) is not the first group to diverge within *Jacarea*, the condition ‘very prominent *canthi rostralii* at maturity (96[1])’ is also explained (see R1, R3, R4, R5, R7 in Figure 10). In those topologies, the clade (*C. yacare* + *C. crocodilus*) is additionally supported by a reversion to the *canthi rostralii* absent or very modest (96[0]). In the R2, R6, R8, R9 and R10 topologies where (*C. yacare* + *C. crocodilus*) is the first group to diverge, the very prominent *canthi rostralii* at maturity (96[1]) is explained by the clade formed by remaining *Jacarea* species (Figure 10).

In the topologies R3, R4, R5 and R7, where (96[1]) is explained by *Jacarea*, the clade within this group is supported by two characters: (1) prefrontals separated by frontals and nasals (128[0]) originated from a population with the prefrontals meeting medially (128[1]); and, (2) the anterior extremity of the frontal is long, reaching or exceeding the anterior margins of the orbits (184[0]), condition derived from a population with short frontal, not reaching the anterior margins of the orbits (184[1]). The frontal condition (184) is only explained in the R3, R4, R5 and R7 topologies (Figure 10), while the prefrontal condition (128) is recovered as synapomorphy of less inclusive groups in trees R6, R8, R9 and R10 (Figure 10).

In the majority of all possible topologies for *Jacarea*, the species *Caiman latirostris* has a close affinity with the genus *Melanosuchus*, being the sister species in R1, R2, R4, R6, R7, R10 (Figure 10), or recovered in a polytomy with UCMP 39978 and *Melanosuchus* on trees R5 and R8 (Figure 10). In the topologies R1, R4 and R7 (Figure 10), the clade (*C. latirostris* + *Melanosuchus*) is supported by two features: (1) the ventral collar scales are displaced in two parallel enlarged rows (45[2]), condition originated and fixed from a population with the ventral collar scales or in a single enlarged row (45[1]); and, (2) the dermal bones of skull roof overhang the rim of supratemporal fenestra near maturity; fenestrae small, with a circular or nearly circular shape (150[1]), condition derived from a population with supratemporal fenestra having a fossa (150[0]). In the trees R2, R6 and R10, the clade (*Caiman latirostris* + *Melanosuchus*) accounts only to the condition (150[1]).

## Exploratory shape analysis

**Dorsal view.** In the principal component analysis from dorsal view, the morphospace with the greatest variance (PC1 vs. PC2) retained ~61% of variance (Figure 11 a) (see Table S3 to remaining components). The PC1 (~46%, Figure 11 a) mainly describes the morphological variations related to: (1) maxilla and jugal contact, along the axis this contact becomes more anterior and medially positioned; (2) the premaxilla and maxilla contact, which becomes



slightly more posterior along this component; (3) maxilla and jugal contact that is positioned more posteriorly and more laterally along the axis, showing the latero-medial compression of the maxilla; (4) lacrimal contact with the maxilla and nasal, becoming slightly more posteriorly positioned; (5) proximal edge of the external nares, that protrudes more laterally in the rostrum; and (6) the contact between premaxilla and nasal, that protrudes to a more distal position in the skull, becoming more anteriorly positioned along the axis of PC1. The projection of individuals in the morphospace occurs along the entire axis of PC1 (Figure 11 a), the individual of *M. latrubessei* retains scores [0.0060161] very close to the scores of the general average of the studied specimens (Table S1), reflecting its morphology, which is similar to the general average for the PC1 (see Table S4 for other scores).

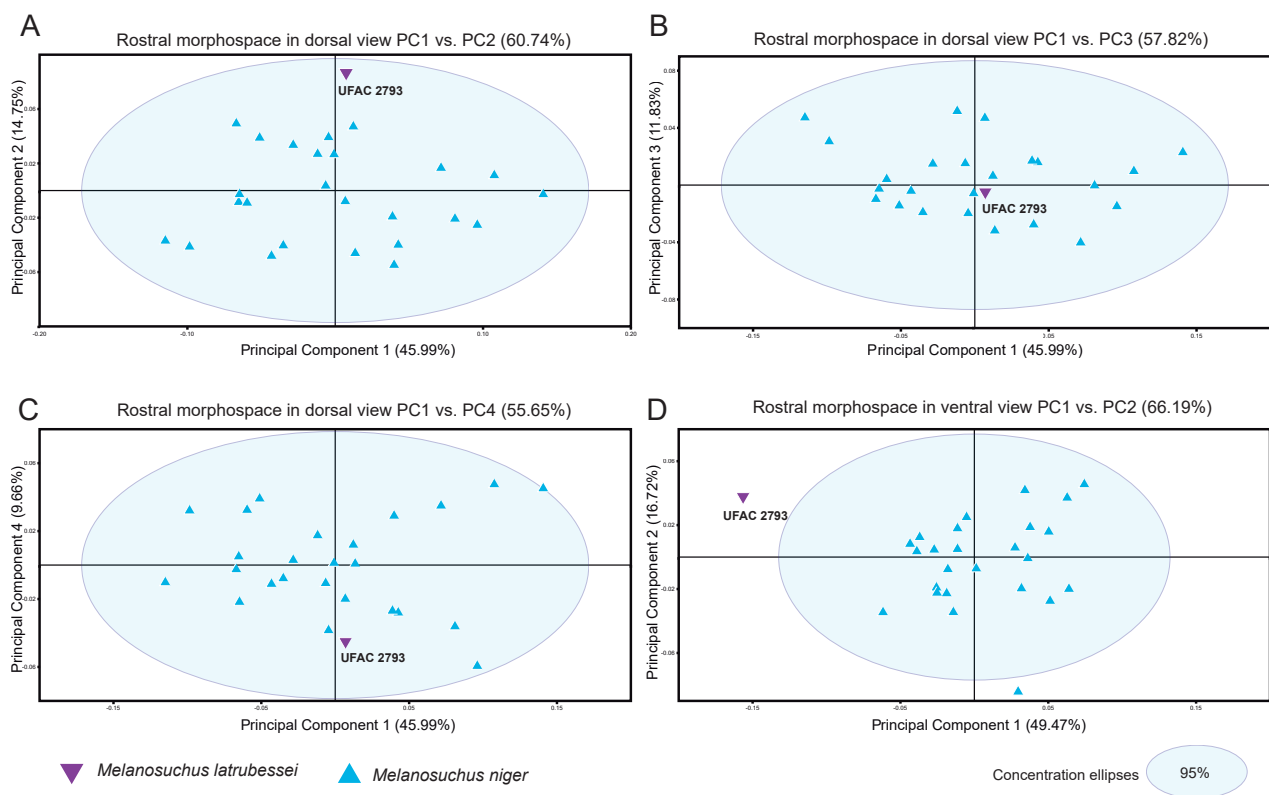
The second component with the greatest variance PC2 (~15%, Figure 11 a) mainly explains the morphological variations related to: (1) antero-posterior shortening of the rostrum and latero-medial expansion of the structure; (2) variations in jugal and maxilla contact, making it more anterior positioned along the axis; (3) the point of greatest lateral expansion of the maxilla becomes slightly posterior, as well as the premaxilla and maxilla contact; (4) contact between jugal, maxilla and nasal, becoming medially located, projecting slightly towards a more posterior portion in the rostrum; (5) medio-lateral expansion of the nasal, and projection of the contact between premaxilla, maxilla and nasal to a more anterior position; and (6) position of the proximal edge of the external nares, which is positioned more medially along the axis of PC2. In the projection of individuals in the morphospace, along the axis PC2, about 6 individuals retain scores similar to the average shape score (see other scores in Table S4), the other individuals are distributed along the entire axis of PC2, summarizing the aforementioned morphological variations for this component. However, unlike the other specimens, *M. latrubessei* has positive scores [0.086004] for PC2 (Figure 11 a), showing that among the studied specimens (Table S1), *M. latrubessei* represents the specimen with the nasal and maxillary expanded laterally, since the PC2 describes these features. Despite of that, it continues to have the point of greatest expansion of the maxilla more posteriorly positioned, the proximal edge of the external nares more medially positioned, and the contact between premaxilla, maxilla and nasal more posteriorly located in the rostrum.

We also evaluated PC3 (~12%), considering that it was above the broken stick, demonstrating that it has statistical significance in relation to the total accumulated variance (see broken stick in Figure S3). When confronted, PC1 vs. PC3 accumulated variance is ~58% (Figure 11 b). PC3 summarizes mainly the changes in morphology retained in: (1) positioning of the suture between premaxilla and maxilla and positioning of the point of greatest expansion of the maxilla in lateral border, where both become more anteriorly located and slightly more lateralized along the component; and (2) positioning of the medial contact between premaxilla and nasal, which extends to a more posterior and slightly more lateral region in the rostrum. For PC3, the distribution of individuals occurs homogeneously throughout the entire component (Figure 11 b); however, it is important to note that *M. latrubessei* presents scores [-0.0053235] very close to the average shape, thus retaining the morphology most similar to the average shape of the samples, differing from the morphology retained at the PC3 axis edges (see Table S4 for scores). The last PC evaluated in this view that showed significant variance based on the broken stick (Figure S3) was the PC4 (~10%). When we evaluate the morphospace generated by confronting PC1 vs. PC4 (Figure 11 c), we observe that there is no overlap between specimens of *M. niger* with the specimen of *M. latrubessei* (Figure 11 c). The PC4 synthesizes variations in the contact between the most anterior portion of lacrimal and anterior region of the posterior chamfered of maxilla, as well as changes in the position of the medial contact between maxilla, lacrimal and nasal. On this axis (PC4, ~10%), the individual of *M. latrubessei* is positioned negatively [-0.046691] (Figure 11 c), thus retaining the shape of the rostrum where contact with the lacrimal and maxilla are further posterior to the rostrum.

**Ventral view.** The morphospace of greatest variance (PC1 vs. PC2) in the analysis of the ventral view retains ~66% of accumulated variance (Figure 11 d) (see Table S5 to remaining components). The axis of greatest variance PC1 (~49%, Figure 11 c) explains mainly morphological variations that are present in: (1) contact between maxilla, ectopterygoid and jugal, which along the axis becomes more anteriorly positioned; (2) lateral contact between palatine and maxilla, which moves to a more anterior and medial portion in the rostrum; (3) anterior and medial contact of the palatine with maxilla, which along the component is positioned at a more anterior point; (4) lateral suture between premaxilla and maxilla, which makes it more medially located; and (5) positioning of the premaxilla and maxilla contact at the medial border of the tooth occlusion pit from the fourth dentary, that moves to a more posterior position in the rostrum. The distribution of individuals in the morphospace, along the PC1, is concentrated closer to the average score, with several individuals retaining slightly negative scores until more positive scores for the PC1 (Figure 11 d). However, differently from that observed in individuals of *M. niger*, the specimen of *M. latrubessei* is positioned at the extreme negative end of the PC1 axis, retaining scores [-0.15751] more extreme than the other

specimens in the studied specimens (Table S1), and therefore spreading distantly from the specimens of *M. niger* in the morphospace (see Table S6 for scores) remaining outside the hypothetical delimitation with the concentration of 95% of the specimens distributed in the morphospace (Figure 11 d). Such projection of *M. latrubessei* mainly reflects the morphology related to the positioning of the posterior contact of the maxilla, ectopterygoid and jugal, but it is also related to the anterior and medial contact of the palatine and maxilla, as well as the position of the suture on the lateral border of the rostrum between premaxilla and maxilla.

The second component with the greatest variance PC2 (~17%, Figure 11 d) summarizes mainly two variations observed in the morphology of the specimens analyzed: (1) position of contact between palatine and maxilla at its most lateral point, which along the axis is positioned more anteriorly and slightly more medially; and (2) position of the labial border of the fourth maxillary alveolus, which along the PC2 varies in the anteroposterior direction. For PC2, *M. latrubessei* presents positive scores [0.037376], summarizing in its distribution in the morphospace characteristics such as the contact between maxilla and palatine more posteriorly located, while the labial border of the 4<sup>th</sup> maxillary tooth is positioned more anteriorly in the rostrum when compared with other specimens of *M. niger* that present more negative scores for this component (Figure 11 d). In this view, we evaluated only the components with the highest variance (PC1 vs. PC2, Figure 11 d), considering that other components remained below the broken stick, and therefore, were disregarded (see broken stick in Figure S4).



**FIGURE 11.** Projection of individuals in the rostral morphospace (PCA). (A) Dorsal view, PC1 vs. PC2 (~61%); (B) Dorsal view, PC1 vs. PC3 (~58%); (C) Dorsal view, PC1 vs. PC4 (~56%); and (D) Ventral view, PC1 vs. PC2 (~66%).

## Discussion

### Phylogenetic and anatomical discussion

The general topology of the strict consensus tree (Figure S1) is in agreement with recent proposition made by Souza-Filho *et al.* (2019). Therefore, the phylogenetic and anatomical discussion, from now on, will be restricted to Jacarea.

The genus *Caiman* was not recovered as monophyletic in the strict consensus and in any of the MLT (SI 3). One of the reasons of polyphyletic in *Caiman* is the species *Caiman gasparinae* being recovered in a polytomy: (*Caiman gasparinae* + *Necrosuchus ionensis* + *Tsoabichi greenriverensis* + *Paleosuchus* + *Mourasuchus* ((UFAC 2507

+ *Purussaurus*) (*Centenariosuchus* + *Jacarea*)). This clade accounts for three characters: (1) the dentary symphysis extends from sixth to eighth alveolus (49[1]), derived from the dentary symphysis extending to fourth or fifth alveolus (49[0]); (2) the maxilla bears broad shelf extending into fenestra, making lateral margin concave (111[1]), derived from the maxilla with linear medial margin adjacent to suborbital fenestra (111[0]); and, (3) dorsal edges of orbits upturned (136[1]), derived from the margin of orbit flush with the skull surface (136[0]). From those, only the dorsal edges of orbits upturned (136[1]) is observed in *Caiman gasparinae*. This condition is observed in all species of the clade, with exception of *Necrosuchus ionensis*, *Melanosuchus latrubessei*, *Mourasuchus pattersoni* Cidade *et al.* 2017, and UCMP 39978, for which it is unknown. All features explained by the more inclusive clades present in this polytomy (characters: 34 [2=>1], 89 [0=>2], 111 [0=>1] {*reversion*}, 150 [1=>0], 186 [0=>1]) are missing in *C. gasparinae* specimens. Therefore, the positioning of *C. gasparinae* outside *Jacarea* could be the consequence of the presence of dorsal edges of orbits upturned (136[1]), that is explained by the aforementioned polytomy, in addition with the missing information regarding all aforementioned features explained by the more inclusive clades. The discovery of new specimens of *C. gasparinae* will be determinant for proper interpretation of those missing characters and understanding of the species phylogenetic relationships.

It is worth to mention that *C. gasparinae* and *Melanosuchus latrubessei* have the nasals excluded from the external nares, with the premaxillaries contacting each other in the dorsal surface (82[2]). However, this condition is homoplastic and originated from populations with nasals contact external nares, but do not bisect it (82[1]) at least ten times independently: *Borealosuchus*, *Boverisuchus magnifrons* Kuhn 1938, *C. gasparinae*, *Diplocynodon*, *Gavialoidea*, *Globidentosuchus*, *Mecistops cataphractus* (Cuvier 1825), *M. latrubessei*, *Mourasuchus* and (*Tomistoma schlegelii* (Müller 1838) + *Thecachampsa Americana* Sellards 1915). The explanation of those homoplastic origins could be related to the intraspecific variability of this condition observed in extant specimens (e.g. *M. niger*), in this way, the homologue hypothesis and species coding must be reviewed by future works. The other condition shared between *C. gasparinae* and species within *Jacarea* is the *canthi rostralii* absent or very modest in mature specimens (96[0]), shared with (*C. crocodylus* + *C. yacare*). However, this is a plesiomorphic condition for *Crocodylia* and two scenarios are possible for the origin and fixation of this feature within *Jacarea*: (1) when (*C. crocodylus* + *C. yacare*) is the first clade within *Jacarea* (Figure 10 R2, R6, R8, R9, R10) this condition is plesiomorphic as observed in *Crocodylia*; (2) when (*C. crocodylus* + *C. yacare*) is not the first clade to diverge within *Jacarea* (Figure 10 R1, R3, R4, R5, R7), this condition is plesiomorphic for *C. gasparinae*, but apomorphic within *Jacarea* being a homoplastic reversion in (*C. crocodylus* + *C. yacare*). Therefore, in any of those scenarios the condition ‘character 96[0]’ can be explained by an exclusive relationship between (*C. crocodylus* + *C. yacare*) with *C. gasparinae*.

The clade (*Caiman crocodylus* + *C. yacare*), in some of the possible results that generated the *Jacarea* polytomy in the strict consensus (Figure 10 R1, R3, R4, R5, R7), accounts for the homoplastic reversion of the character 96[0] as earlier mentioned. However, in all MLT this clade is supported by two other features: (1) the species have surangulars with a spur bordering the dentary tooth row lingually ranging from at least one alveolus (62[0]), feature derived from the lack of such spur (62[1]); and (2) the clade has an occlusion pit between seventh and eighth maxillary teeth with all other dentary teeth occlude lingually (92[1]), derived from condition in which all dentary teeth occluding lingually to the maxillary teeth (92[0]). Both of those characters are homoplastic, being the character 62[0] independently shared with *Borealosuchus sternbergii* Gilmore 1910, (*Gavialis gangeticus* (Gmelin 1789) + *Gryposuchus colombianus* (Langston 1965)), *Mecistops cataphractus*, and (*Tomistoma schlegelii* + *Thecachampsa americana*). The character 92[1] is homoplastic shared with *B. sternbergii*, ‘*Crocodylus affinis*, *Diplocynodon hantoniensis* (Wood 1846), and *Planocrania hengdongensis* Li 1984. As all the possible characters explained by (*C. crocodylus* + *C. yacare*) are homoplastic in some degree, we cannot argue that the topologies where character 96[0] is reverted for the group (Figure 10 R1, R3, R4, R5, R7) are less plausible than the plesiomorphic condition observed in the other results (Figure 10 R2, R6, R8, R9, R10). Earlier works have found (*C. crocodylus* + *C. yacare*) as the first clade to diverge (e.g. Brochu 1999, 2011; Fortier *et al.* 2014), while other analyses recovered it within a polytomy, as in the present work (e.g. Cidade *et al.* 2020; Souza-Filho *et al.* 2019). As such, the position of this clade within *Jacarea* remains an open debate.

The species *Caiman wannlangstoni* occupies two main positions on the possible recovered trees for *Jacarea*: (1) as the first clade to diverge (Figure 10 R3, R5, R7, and including R4, where UCMP 39978 forms a polytomy in the base of the clade); (2) as a species from the second divergent branch (Figure 10 R2, R6 and R8). When *C. wannlangstoni* is the first clade to diverge, *Jacarea* accounts for character 96[1] (including the already discussed reversion in (*C. crocodylus* + *C. yacare*)) and character 111[1]. In this context, the second clade to diverge is sup-



ported by character 128[0] and 184[0], which in the strict consensus cladogram has an ambiguous reconstruction for Jacarea by two factors: (1) *Centanariosuchus gilmorei* is unknown for both conditions; (2) there are species within Jacarea accounting for the two variations of both homologues. Therefore, when *C. wannlangstoni* is the first clade to diverge (including when UCMP 39978 forms a polytomy there, in Figure 10 R4, by also being unknown for both conditions), the prefrontals meeting medially (128[1]) and the anterior extremity of the frontal being short, without reaching the anterior margins of the orbits (184[1]), become the plesiomorphic condition for Jacarea.

Thus, in the second clade to diverge (Figure 10 R2, R4, R6 and R8), both conditions are reverted to prefrontals separated by frontals and nasals (128[0]) and the anterior extremity of the frontal long (184[0]). In *C. yacare* the prefrontals meeting medially (128[1]) is secondarily reverted from an ancestral with prefrontals separated by frontals and nasals (128[0]). In the evolutionary scenario where *C. wannlangstoni* belongs to the second clade to diverge (Figure 10 R2, R6 and R8), this clade is supported by the already discussed character 96[1]. Also, the less inclusive clade posterior to the one including *C. wannlangstoni* accounts for the origin and fixation of character 128[0]. However, in this context 128[1] also originated independently in *C. yacare*. Therefore, considering those possible evolutionary scenarios the discovery of new and more complete specimens of *Centanariosuchus gilmorei* will help to understand the early condition of Jacarea for characters 128 and 184.

The species *C. brevirostris* is always included in the clade accounting for the character 128[0], usually being nested within the sister clade of (*C. latirostris* + *Melanosuchus*) (Figure 10). Only in one topology *C. brevirostris* is undoubtedly the sister species of (*C. latirostris* + *Melanosuchus*) (Figure 10 R6).

The species *Caiman latirostris* was recovered as the sister species of *Melanosuchus* (Figure 10 R1, R2, R4, R6, R7 and R10) or nested within the clade that includes *Melanosuchus* forming a polytomy (Figure 10 R3, R5, R8 and R9). The character ventral collar scales in two parallel enlarged rows (45[2]) derived from the ventral collar scales in a single enlarged row (45[1]) supports the relationship of *C. latirostris* as the sister species of the *Melanosuchus* genus only in topologies where (*C. crocodilus* + *C. yacare*) is not the first clade to diverge within Jacarea (Figure 10 R1, R4, R7). As this condition is unknown in UCMP 39978, the topologies where a polytomy is formed between *C. latirostris*, *Melanosuchus* and UCMP 39978 and in which the (*C. crocodilus* + *C. yacare*) is not the first clade to diverge within Jacarea, it is also supported by the aforementioned condition (i.e. character 45[2]; Figure 10 R5). In topologies with (*C. crocodilus* + *C. yacare*) being the first clade to diverge within Jacarea (Figure 10 R2, R6, R8 and R10, including the topology R3), there is not enough evidence to infer the plesiomorphic condition of the clade. This occurs because this feature is only known for extant species, with (*C. crocodilus* + *C. yacare*) expressing the character 45(1) and (*C. latirostris* + *Melanosuchus*) expressing the character 45(2).

The topologies where (*C. latirostris* + *Melanosuchus*) is observed (Figure 10 R1, R2, R4, R6, R7 and R10) including when UCMP 39978 forms a polytomy with *C. latirostris* and *Melanosuchus* (Figure 10 R5 and R8), account for a linear frontoparietal suture (150[1]), derived from a population with concavo-convex frontoparietal suture (150[0]). Within Jacarea this condition is unknown for *M. latrubessei* and UCMP 39978, while the remaining species exhibit a concavo-convex suture (150[0]). Therefore, the linear suture in (*C. latirostris* + *Melanosuchus*) is a reversion within Jacarea for the early condition in Caimaninae, while being homoplastically shared with several other Crocodylia. The discovery of more complete specimens specifically related with UCMP 39978 that elucidate the condition of the frontoparietal suture (150) will help to clarify the affinities of this specimen with *C. latirostris* + *Melanosuchus*.

The relationship between *Caiman latirostris* and *Melanosuchus* genus is not a novelty in the literature. This relationship was recovered in most phylogenetic inferences based on morphological data (e.g. Brochu 1999, 2011; Salas-Gismondi *et al.* 2015; Hastings *et al.* 2016; Souza-Filho *et al.* 2019). However, in molecular data analyses, *Melanosuchus* appears as sister clade of the extant *Caiman* (e.g. Poe 1996; Oaks 2011).

As it was already mentioned, the genus *Melanosuchus* accounts in all possible trees for the vomer being exposed on palate at premaxilla–maxilla suture (99[1]). It is important to remark that *M. latrubessei* has the nasals excluded, at least externally, from the external nares, thus the premaxillae contact each other on the dorsal surface (82[2]) as in *C. gasparinae*, but different from remaining Jacarea species.

The ten different topologies that generated the polytomy in the strict consensus cladogram were the result of the different positioning of the specimen UCMP 39978. Therefore, this specimen can be considered a wild-card taxon within the clade Jacarea, playing an important role in reducing the resolution of the group.

There are some homologs with the potential to be included in future phylogenetic inferences, namely: (1) the anterior limit of the suborbital fenestra in relation to the maxillary alveoli; (2) the length of the anterior process of

ectopterygoid bordering the lateral margin of the suborbital fenestra in relation to the maxillary alveoli (which can be biologically dependent with character 185 from Brochu (2013)); and, (3) the range of the posterior premaxillary process, in ventral view, in relation to the maxillary alveoli. The homolog 1 and 2 are based on the relative positioning relative to the posterior maxillary alveoli. As discussed earlier, the variation on the alveolar number of the maxillae seems to occur at the posterior portion of the tooth row with inclusion or reabsorption of maxillary alveoli. Therefore, further studies improving the basis of those proposed homolog should be made with the intention to refine and solve the problems derived from the maxillary alveoli count.

### Geometric Morphometrics of *Melanosuchus rostrum*

Through the analysis of geometric morphometrics, it was possible to explore the morphological variations present in the rostrum of *M. niger* in contrast to the morphology of *M. latrubessei*. Through the analysis in dorsal view, we note that the main variations in morphology are related to the contact of the maxilla and jugal; suture between premaxilla and maxilla; maxilla and jugal contact; suture between lacrimal with the maxilla and nasal; the proximal edge of the external nares and, finally, to the contact between premaxilla and nasal. *M. latrubessei*, in dorsal view, represents the specimen with the greatest lateral maxillary and nasal expansion, and also presenting the point of greatest expansion of the maxilla more posteriorly positioned, beyond the proximal edge of the external nares more medially positioned, as well as the contact between premaxilla, maxilla and nasal more previously located in the rostrum. It is interesting to note that in a previous study developed by Foth *et al.* (2015) exploring the cranial geometry of *M. niger*, they present as results that the main variations in the morphology of *M. niger* related to the rostrum are concentrated in the length and depth of this structure and are related to the ontogeny of the specimens (see Foth *et al.*, 2015). Our analyses found similar results, but were developed only with specimens in a more advanced ontogenetic stage.

Inventral view, we notice that the greatest variations are present in the contact between maxilla, ectopterygoid and jugal; in the lateral contact between palatine and maxilla; in the anterior and medial contact of the palatine with maxilla; on the lateral suture between premaxilla and maxilla; and finally at the positioning of the premaxilla and maxilla contact at the medial border of the tooth mark from the fourth dentary. *M. latrubessei* reflects the morphology related to the positioning of the posterior contact of the maxilla, ectopterygoid and jugal, also related to the anterior and medial contact of the palatine and maxilla, as well as the position of the suture on the lateral border of the rostrum between premaxilla and maxilla. These morphological characteristics differ greatly from what is observed in all *M. niger* specimens studied. As the work of Foth *et al.* (2015) does not evaluate variations of *M. niger* in the ventral view of the skull, future works focusing on this view may shed light on morphological variations aspects of this genus. However, as expressed in the results of geometric morphometry, *M. latrubessei* occupies different positions in the morphospace than those occupied by the *M. niger* specimens (Figure 11), therefore suggesting a significant variation in the morphology of the palatal region between these two species, highlighting with quantitative morphology some of the diagnoses aforementioned for *M. latrubessei*. In addition, we comment that *M. latrubessei* presents differences in rostral morphology that differ from those intraspecific variations observed in *M. niger*.

### Inference on paleoecology

The only known specimen of *Melanosuchus latrubessei*, UFAC 2793, corresponds to a mature individual based on the well-developed rostral ridges and size, being proportional to the medium-sized *M. niger* specimens studied (see Table 1). The similarities between these two *Melanosuchus* species are not restricted to size, with both exhibiting large rostrums and with, at least, the most posterior maxillary teeth presenting short crowns convex apex (blunted or globular teeth). Therefore, it is reasonable to assume that *M. latrubessei* was able to prey, during adulthood, organisms similar to those observed for *M. niger*, such as fish, reptiles (including other crocodylians and small and medium turtles), and small to medium mammals (Rueda-Almonacid *et al.* 2007; Blanco *et al.* 2014). In addition, for large prey, the 'death roll' is expected and possible, based on the morphological similarities of *M. latrubessei* and *M. niger* (see Blanco *et al.* 2014 to 'death roll').

To date, the Solimões Formation has seven Crocodyliformes species described, plus one longirostrine morphotype attributed to *Hesperogavialis* sp. (Riff *et al.* 2010). *Caiman brevirostris* is a small to medium-sized crocodylian more adapted for durophagous feeding (Fortier *et al.* 2014). *Gryposuchus jessei* and *Hesperogavialis* sp. are medium to large-sized longirostrine gavialoids, better interpreted as piscivorous of different sizes of fish. Other longirostrine taxon is *Charactosuchus* (Crocodyloidea), which is a small to medium size animal, with very thin and gracile mandibles, thus being probably a piscivorous of small fish or a predator of other small animals (e.g., mol-

lusk, crustaceans). *Mourasuchus amazonensis* and *Mourasuchus arendsi* are large-sized crocodylians that were able to prey several small animals, such as crustaceans and mollusks, without the help of teeth, using the long, large and thin mandibles using the ‘gulp-feeding’ as a feeding strategy (Cidade *et al.* 2017, 2019b). The Caimaninae *Purussaurus brasiliensis* was a large hypercarnivore (Aureliano *et al.* 2015), which could prey large sized mammals such as toxodonts, rodents (*Phoberomys*) and large turtles such as *Stupendemys* and *Podocnemys*. Also, it is probable that the juvenile individuals of *Purussaurus* played a similar role as the one occupied by small to medium-sized generalist crocodylians, such as the extant *Caiman* species and *Paleosuchus*.

To date, the Talismã locality has a remarkable diversity of fauna recovered, composed mainly by: *Charactosuchus* (Crocodyloidea; Souza-Filho & Bocquentin-Villanueva 1989; Souza-Filho 1993); Litopterna (Proterotheriidae), Rodentia (Neopiblemidae), Agoutidae indet., Primates indet., and Atelidae indet. (Bergqvist *et al.* 1998); *Chelus* sp. (Bocquentin *et al.* 2001); *Octodontobradys puruensis* Santos *et al.* 1993 (Xenarthra; Orophodontidae), *Potamarchus murinus* Burmeister 1885 (Rodentia), *Neopiblema horridula* Ameghino 1889 (Rodentia), and cf. *Caiman brevirostris* (Alligatoridae; Cozzuol 2006); *Eunectes* (Boidae) and cf. *Eunectes* (Boidae; Hsiou & Albino 2009); cf. *Paradracena* (Scleroglossa: Teiidae; Hsiou *et al.* 2009); *Colombophis spinous* Hsiou *et al.* 2010 (Alethinophidia; Hsiou *et al.* 2010); cf. *Hapalops* (Xenarthra; Megalonychidae), cf. *Planops* (Xenarthra; Megatheriidae), and Primates indet. (Negri *et al.* 2010); *Octodontobradys* (Xenarthra; Orophodontidae; Guilherme *et al.* 2011); *Caiman brevirostris* (Fortier *et al.* 2014); invertebrates, fish fragments, *Mourasuchus* remains, Gavialoidea remains and Anhingidae birds (Souza-Filho & Guilherme 2015); *Potamarchus* sp. (Rodentia; Dinomyidae; Kerber *et al.* 2016); and, *Acerosuchus pachytemporalis* (Souza-Filho *et al.* 2019). Those listed fossils were collected from two fossiliferous levels, one at 1.7 m and the other 7 m above the water level (Cozzuol 2006). However, the major portion of the collected specimens have no stratigraphic horizon discrimination, turning difficult the proper diversity comparison between those levels.

The Talismã locality is here interpreted as an almost abandoned meander, with slow contribution of water and, consequently, with thin sediments originating from the main river. This can be evidenced by the presence of fine-grained sediments (e.g. silts and clays), absence of horizontal lamination and the thinning-up profile of the rocks in the section. Despite the distance between the two fossiliferous facies and, consequently, the difference in their ages, it is reasonable to assume that the temporal difference and the time average of these facies are smaller in relation to the fossils deposited in meandering channels (see Souza *et al.* 2016 for briefly discussion). Therefore, we can assume an aging difference between the facies estimated in few thousands of years, which enable the coexistence in time and space between the species recovered from Talismã locality.

Based on the Crocodylia specimens from the Talismã locality, there are at least two longirostrine of different sizes: the small *Charactosuchus* sp. and the medium to large-sized Gavialoidea indet. The *Mourasuchus* sp. and the durophagous *Caiman brevirostris* represent taxa that ate several small specimens, such as crustaceans and mollusks. *Melanosuchus latrubessei* represents a medium-sized generalist predator. Despite the absence of *Purussaurus* remains, the presence of this taxon cannot be ruled out, as well as the presence of other medium-sized predators such as other species of *Caiman*.

In the context of the Talismã locality having originated from an almost abandoned meander, the intensity of this connection with the main river seems to vary along the existence of this meander. In this way, the water flux, at this region, was slow but constant, enabling fish and other animals to transit between this meander and the main river course. As consequence of the water flux, it is probable that the meander water was perennially filled with sediments, thus becoming blurred as a result. This locality seems to present at least three different habitats: (1) the mainstream and its connection with the meander; (2) the margins of the meander; and (3) the deepest portions of the meander. All species probably inhabited the niches 1 and 2.

The coexistence between the aforementioned species is defended here, but they could have used this meander differently along the seasons of the year, for example with large specimens only inhabiting the niches 2 and 3 when the meander was full. The coexistence of those species in this simple environment seems reasonable based on the differences on the inferred feeding behavior, mainly related with the rostrum shape as adaptations for different foraging modes (Pooley & Gans 1976; Magnusson *et al.* 1987). It is common to observe rostrum differences when two species coexist (Dodson 1975). The overlap of niche occupation and feeding resources between the generalist crocodylians, such as *Gryposuchus*, *Hesperogavialis* and *Charactosuchus*, is unavoidable. However, this overlap does not prevent the coexistence of these species, and the coexistence of different species of extant Caimaninae support this (e.g. Grigg & Kirshner 2015).



The extant *Caiman crocodilus* and *Melanosuchus niger* present an overlapping distribution, being found together in rivers, lakes, and channels throughout Amazonia biome (Medem 1963; Magnusson 1985; Herron 1994; Brazaitis *et al.* 1996; Silveira *et al.* 1997; Aguilera *et al.* 2008; Marioni *et al.* 2008; Grigg & Kirshner 2015). Both species prey on terrestrial invertebrates at an early age before switching to mollusks, fish and some terrestrial vertebrates as they grow (Magnusson *et al.* 1987). The sharing of the same habitat for large populations of both species is only possible due to the difference in microhabitats preference observed between them. For example, *M. niger* occurs most commonly near steep banks with little floating grass, while *C. crocodilus* occurs most frequently in shallow or grassy areas (Magnusson 1985). Also, this segregation is associated with individual size variation and could reflect the exclusion of one species by the other from microhabitats preferred by both or an interspecific difference in microhabitat preference (Herron 1994). Therefore, it is reasonable to expect a similar scenario of differential microhabitat preference between medium-sized predators, such as *Acerosuchus pachytemporalis* and *M. latrubessei*, for example.

### Comments on the *Melanosuchus* evolution

Based on previous morphological phylogenetic inferences (e.g. Poe 1996; Brochu 1999, 2011; Salas-Gismondi *et al.* 2015; Hastings *et al.* 2016; Souza-Filho *et al.* 2019) and the present work resolutions for Jacarea polytomy (Figure 10), it is plausible to assume *Caiman latirostris* as the sister species of *Melanosuchus* genus. In this context, *Caiman* is non-monophyletic by the exclusion of *Caiman gasparinae* and by the presence of *Melanosuchus* species within the clade. Therefore, based only on the present results, a new genus should be erected for *C. gasparinae* and, for the sake of the *Caiman* monophyletism, the genus *Melanosuchus* should be synonymized with *Caiman*, making Jacarea redundant with this genus. However, the present work will refrain from making these changes waiting for more profound revisions on the species and for better resolved phylogenetic inferences.

The oldest occurrences of *Caiman latirostris* are from the late Miocene formations Ituzaingó, in Argentina (Bona *et al.* 2013a) and Urumaco, in Venezuela (Bona *et al.* 2013a; Scheyer & Delfino 2016), together with specimens tentatively referred as *Caiman* cf. *C. latirostris* from the Miocene of Argentina, Palo Pintado Formation (Salta Province; Starck & Anzotequi 2001; Bona *et al.* 2014). Those oldest occurrences of *C. latirostris* species are in agreement with the actual distribution of the species, which ranges from Argentina, Paraguay, Bolivia, Uruguay and the drainage basins of the southeastern coast of Brazil (Grigg & Kirshner 2015). As mentioned previously, the oldest occurrences of the genus *Melanosuchus* are also from the Miocene, but from the northmost portions of South America and in agreement with the distribution of extant *Melanosuchus niger* (Grigg & Kirshner 2015). Therefore, based on phylogenetic inferences, if *C. latirostris* is the sister species of the ancestral of *M. niger*, we can estimate a divergence between these species between the early Miocene and the late Oligocene (based on the assumption that the ancestor species existed necessarily in geological periods prior to the oldest occurrences of such sister species). Also, current and past distributions of these species favor an unspecified vicariance event, splitting the common ancestral population between *C. latirostris* and *Melanosuchus* in two, with *C. latirostris* occupying the southernmost portions and *Melanosuchus* the northernmost portions of South America. This vicariance event may be related with the development of the Chaco region (e.g. Morrone 2013).

Assuming that the holotype of *Melanosuchus fisheri* is in fact a specimen of *M. niger* (Bona *et al.* 2017b; Foth *et al.* 2017) the oldest record of both *Melanosuchus* species are from the late Miocene, with *M. niger* being from Urumaco Formation, in Venezuela, and *M. latrubessei* from Solimões Formation, in Brazil. As there is no evidence of both species co-occurring in the same environments at the same time and upon the fact that one species occurs in a more northern area than the other, it is reasonable to assume an unspecified vicariance event that split the ancestral population of the genus in two. Recently, post-cranial elements material attributed to *Melanosuchus* cf. *M. niger* have been described and the specimen must be properly assigned to one of the *Melanosuchus* species, since there are no relevant morphometric differences between the fossil and specimens of *M. niger* in addition to other morphological features (Lacerda *et al.* 2018, 2020); however, only new findings of more complete and comparable specimens will allow this specific distinction. If this post-cranial bone is in fact a *M. niger*, such presented hypothesis must be reviewed, and both species probably shared the same environments. However, if the described specimens in Lacerda *et al.* (2020) is latter recognized as an *M. latrubessei*, the vicariant hypothesis proposed here is corroborated. If the inferences proposed here are right, this split must have occurred sometime after the *Caiman latirostris* and *Melanosuchus* genus split. However, further studies regarding the phylogenetic inferences and the fossil occurrences in other ages of those species are necessary for a better understanding of these species' evolution.

The extinction of the Miocene-Pliocene faunas of the Solimões Formation, including *Melanosuchus latrubessei*, seems to be directly related with the uplift of the northern portions of the Andes, which generated significant changes in drainages and Amazon environments (Hoorn *et al.* 2010, 2017; Horbe *et al.* 2019). Major environmental changes in short periods of time are enough to lead to the extinction of fauna and floristic components of the affected environment (e.g. Riff *et al.* 2010; Scheyer *et al.* 2013; Souza-Filho *et al.* 2014).

It is important to note that, in this context, the populations of *Melanosuchus niger* from Venezuela have not been extinct in Neogene, as it seems to have happened with *M. latrubessei*, enabling the subsequent colonization of the Amazon region by *M. niger*, leading to the current pattern of distribution of the species. This could indicate a differential extinction pressure between *M. latrubessei* and *M. niger*, or perhaps an adaptability of *M. niger* to environmental changes, both of which are not yet explained.

## Conclusion

The new species *Melanosuchus latrubessei* increases the already high crocodyliform diversity in the Neogene of the Solimões Formation. This is the first cranial occurrence of the genus for this Formation, bringing important information regarding the evolution of the genus, as well as about the Caimaninae clade as a whole. *M. latrubessei* seems to have been a medium-sized generalist species that coexisted in the drainages of the Solimões Formation with other medium to large-sized generalist crocodylians, such as *Caiman* and *Purussaurus*. This reinforces the spread of microhabitats and food resources for the proto-Amazon recorded in the rocks of Solimões Formation. This work brings other important questions to be answered in the future, such as improvements of Jacarea's phylogenetic hypotheses and key questions about how the extant *Melanosuchus* species and its ancestral genus originated, as well as on the biogeography of *Melanosuchus*.

## Acknowledgments

The authors wish to thank: Dr. Jean C. Bocquentin and Dr. Alceu Ranzi for collaboration and invaluable efforts during the field works at Amazonian rivers; to Philipe M. Ferreira (MN/UFRJ), for help in vomer discussion, providing important commentaries and references about Squamata; to Kamila L. N. Bandeira (MN/UFRJ) and Rodrigo V. Pêgas (UFABC), for useful commentaries in the manuscript draft; to Camila B. Pinto (UFMG), for the grammar review of the manuscript draft. The authors also wish thanks to the Willi Hennig Society, for making TNT a free access program. Additionally, to the following curators who gave us access to studied specimens: Matthew A. Brown and James C. Sagebiel (TMM); Luciana B. Carvalho and Manoela W. Cardoso (MNRJ); Kevin Queiroz, Kenneth A. Tighe and Addison Wynn (USNM); David A. Kizirian and Lauren Vonnahme (AMNH); Diógenes A. Campos and Rodrigo Machado (MCT); David C. Blackburn and Coleman M. Sheehy III (UF); Alan Resetar (FMNH); Gunther Köhler (SMF); and Frank Glaw (ZS). We thank Christopher Brochu (University of Iowa) and the anonymous reviewers for suggestions that made it possible to improve the manuscript. The author LGS thanks to Coordenação de Aperfeiçoamento de Pessoal de Nível Superior (CAPES) for Ph.D scholarship [88882.183263/2018-01], Fundação de Amparo à Pesquisa do Estado do Amazonas (FAPEAM) for the posdoctorate scholarship [062.00166/2020], and to financial support granted to Paleo/Geohistory exhibition at Museu da Amazônia [PRONAC 183808]; GMC thanks the Conselho de Desenvolvimento Científico e Tecnológico (CNPq) [40808/2016-7] and CAPES [Finance Code 001]; MBSL thanks for the support granted by CAPES for Ph.D scholarship [88882.381382/2019-1].

## References

- Adams, D.C., Rohlf, F.J. & Slice, D.E. (2013) A field comes of age: geometric morphometrics in the 21<sup>st</sup> century. *Hystrix, the Italian Journal of Mammalogy*, 24 (1), 1–8.  
<https://doi.org/10.4404/hystrix-24.1-6283>
- Aguilera, O.A. (2004) *Tesoros Paleontológicos de Venezuela: Urumaco, patrimonio natural de la humanidad*. Editora Arte, Caracas, 148 pp.
- Aguilera, O.A., Riff, D. & Bocquentin-Villanueva, J. (2006) A new giant *Purussaurus* (Crocodyliformes, Alligatoridae) from the

- upper Miocene Urumaco Formation, Venezuela. *Journal of Systematic Paleontology*, 4 (3), 221–232.  
<https://doi.org/10.1017/S147720190600188X>
- Aguilera, X., Coronel, J.S., Oberdorff, T. & Damme, P.A.V. (2008) Distribution patterns, population status and conservation of *Melanosuchus niger* and *Caiman yacare* (Crocodylia, Alligatoridae) in oxbow lakes of the Ichilo river floodplain, Bolivia. *Revista de Biología Tropical*, 56 (2), 909–929.  
<https://doi.org/10.15517/rbt.v56i2.5633>
- Aureliano, T., Ghilardi, A.M., Guilherme, E., Souza-Filho, J.P., Cavalcanti, M. & Riff, D. (2015) Morphometry, bite-force, and paleobiology of the Late Miocene Caiman *Purussaurus brasiliensis*. *Plos One*, 10 (2), e0117944.  
<https://doi.org/10.1371/journal.pone.0117944>
- Avery, D.F. & Tanner, W.W. (1971) Evolution of the iguanine lizards (Sauria, Iguanidae) as determined by osteological and myological characters. *Brigham Young University Science Bulletin, Biological Series*, 12 (3), 1–89.
- Barbosa-Rodrigues, B. (1892) Les Reptiles fossils de la vallée de l'Amazone. *Vellosia*, 2, 41–46.
- Benton, M.J. & Clark, J.M. (1988) Archosaur phylogeny and the relationships of the Crocodylia. In: Benton, M.J. (Eds.), *The Phylogeny and Classification of the Tetrapods. Vol. 1. Amphibians, Reptiles, Birds*. Clarendon Press, New York, pp. 295–338.
- Bergqvist, L.P., Ribeiro, A.M. & Bocquentin-Villanueva, J. (1998) Primata, Roedores e Litopternas do MioPlioceno da Amazônia Sul-Occidental. *Geologia Colombiana*, 23, 19–29.
- Bissaro-Júnior, M.C., Kerber, L., Crowley, J.L., Ribeiro, A.M., Ghilardi, R.P., Guilherme, E., Negri, F.R., Souza-Filho, J.P. & Hsiou, A.S. (2019) Detrital zircon U-Pb geochronology constrains the age of Brazilian Neogene deposits from Western Amazonia. *Palaeogeography, Palaeoclimatology, Palaeoecology*, 516, 64–70.  
<https://doi.org/10.1016/j.palaeo.2018.11.032>
- Blanco, R.E., Jöner, W.W. & Villamil, J. (2014) The ‘death roll’ of giant fossil crocodyliforms (Crocodylomorpha: Neosuchia): allometric and skull strength analysis. *Historical biology*, 27 (5), 514–524.  
<https://doi.org/10.1080/08912963.2014.893300>
- Bocquentin, J., Guilherme, E. & Negri, F.R. (2001) Duas espécies do gênero *Chelus* (Pleurodira, Chelidae) no Mioceno Superior-Plioceno da Amazônia Sul-Occidental. *Geociências*, 6 (6), 50–55.
- Bocquentin-Villanueva, J. (1984) Um nuevo Nettosuchidae (Crocodylia, Eusuchia) proveniente de la Formación Urumaco (Mioceno Superior), Venezuela. *Ameghiniana*, 21, 3–8.
- Bona, P. & Barrios, F. (2015) The Alligatoroidea of Argentina: an update of its fossil record. In: Fernández, M. & Herrera, Y. (Eds.), *Reptiles Extintos - Volumen en Homenaje a Zulma Gasparini. Publicación Electrónica de la Asociación Paleontológica Argentina*, 15 (1), pp. 143–158.
- Bona, P. & Carabajal, A.P. (2013) *Caiman gasparinae* sp. nov., a huge alligatorid (Caimaninae) from the late Miocene of Paraná, Argentina. *Alcheringa*, 37 (4), 462–473.  
<https://doi.org/10.1080/03115518.2013.785335>
- Bona, P., Degrange, F.J. & Fernández, M.S. (2013a) Skull anatomy of the bizarre crocodylian *Mourasuchus nativus* (Alligatoridae, Caimaninae). *The anatomical record*, 296 (2), 227–239.  
<https://doi.org/10.1002/ar.22625>
- Bona, P. & Desojo, J.B. (2011) Osteology and Cranial Musculature of *Caiman latirostris* (Crocodylia: Alligatoridae). *Journal of Morphology*, 272 (7), 780–795.  
<https://doi.org/10.1002/jmor.10894>
- Bona, P., Riff, D. & Gasparini, Z. (2013b) Late Miocene crocodylians from Northeast Argentina: new approaches about the austral components of the Neogene South American crocodylian fauna. *Earth and Environmental Science: Transactions of the Royal Society of Edinburgh*, 103 (3–4), 551–570.  
<https://doi.org/10.1017/S175569101300042X>
- Bona, P., Starck, D., Galli, C., Gasparini, Z. & Reguero, M. (2014) *Caiman cf latirostris* (Alligatoridae, Caimaninae) in the late Miocene Palo Pintado Formation, Salta Province, Argentina: paleogeographic and paleoenvironmental considerations. *Ameghiniana*, 51, 26–36.  
<https://doi.org/10.5710/AMEGH.11.12.2013.1507>
- Bona, P., Paulina-Carabajal, A. & Gasparini, Z. (2017a) Neuroanatomy of *Gryposuchus neogaeus* (Crocodylia, Gavialoidea): A first integral description of the braincase and endocranial morphological variation in extinct and extant gavialoids. *Earth and Environmental Science Transactions of the Royal Society of Edinburgh*, 106 (4), 235–246.  
<https://doi.org/10.1017/S1755691016000189>
- Bona, P., Fernandez-Blanco, M.V., Scheyer, T.M. & Foth, C. (2017b) Shedding light on the taxonomic diversity of the South American Miocene caimans: the status of *Melanosuchus fisheri* (Crocodylia, Alligatoroidea). *Ameghiniana*, 54, 681–687.  
<https://doi.org/10.5710/AMGH.08.06.2017.3103>
- Brazaitis, P., Rebêlo, G.H. & Yamashita, C. (1996) The status of *Caiman crocodilus crocodilus* and *Melanosuchus niger* populations in the Amazonian regions of Brazil. *Amphibia-Reptilia*, 17, 377–385.  
<https://doi.org/10.1163/156853896X00090>
- Brochu, C.A. (1997) Fossils, morphology, divergence timing, and the phylogenetic relationships of *Gavialis*. *Systematic Biology*, 46, 479–522.  
<https://doi.org/10.1093/sysbio/46.3.479>



- Brochu, C.A. (1999) Phylogenetics, taxonomy, and historical biogeography of Alligatoroidea. *Journal of Vertebrate Paleontology*, 19, 9–100.  
<https://doi.org/10.1080/02724634.1999.10011201>
- Brochu, C.A. (2011) Phylogenetic relationships of *Necrosuchus ionensis* Simpson, 1937 and the early history of caimanines. *Zoological Journal of the Linnean Society*, 163 (Supplement 1), S228–S256.  
<https://doi.org/10.1111/j.1096-3642.2011.00716.x>
- Brochu, C.A. (2013) Phylogenetic relationships of Palaeogene ziphodont eusuchians and the status of *Pristichampsus* Gervais, 1853. *Earth and Environmental Science Transactions of the Royal Society of Edinburgh*, 103 (3–4), 521–550.  
<https://doi.org/10.1017/S1755691013000200>
- Campos, D.A., Alves, E.D.O. & Campos, D.R.B. (1976) Localidades fossilíferas da Folha SC.19 Rio Branco. In: Silva, L.L., Rivetti, M., Del'arco, J.O., Almeida, L.F.G., Dreher, A. M. & Tassinari, C.C.G. (Eds.), *Geologia. Projeto RadamBrasil*, Rio de Janeiro, Levantamento de recursos naturais 12, pp. 65–79.
- Chandless, W. (1866) Ascent of the River Purûs. *Journal of the Royal Geographical Society of London*, 36, 86–118.
- Cidade, G.M., Fortier, D. & Hsiou, A.S. (2019a) The crocodylomorph fauna of the Cenozoic of South America and its evolutionary history: a review. *Journal of South American Earth Sciences*, 90, 392–411.  
<https://doi.org/10.1016/j.jsames.2018.12.026>
- Cidade, G.M., Riff, D. & Hsiou, A.S. (2019b) The feeding habits of the strange crocodylian *Mourasuchus* (Alligatoroidea, Caimaninae): a review, new hypotheses and perspectives. *Revista Brasileira de Paleontologia*, 22 (2), 106–119.  
<https://doi.org/10.4072/rbp.2019.2.03>
- Cidade, G.M., Solórzano, A., Rincón, A.D., Riff, D. & Hsiou, A.S. (2017) A new *Mourasuchus* (Alligatoroidea, Caimaninae) from the late Miocene of Venezuela, the phylogeny of Caimaninae and considerations on the feeding habits of *Mourasuchus*. *PeerJ*, 5, e3056.  
<https://doi.org/10.7717/peerj.3056>
- Cidade, G.M., Solórzano, A., Rincón, A.D., Riff, D. & Hsiou, A.S. (2020) Redescription of the holotype of the Miocene crocodylian *Mourasuchus arendsi* (Alligatoroidea, Caimaninae) and perspectives on the taxonomy of the species. *Historical Biology*, 32 (6), 733–749.  
<https://doi.org/10.1080/08912963.2018.1528246>
- Cunha, P.R.C. (2007) Bacia Acre. *Boletim Geociências Petrobras*, 15 (2), 207–215.
- Cooke, S.B. & Terhune, C.E. (2015) Form, Function, and Geometric Morphometrics. *The Anatomical Record*, 298, 5–28.  
<https://doi.org/10.1002/ar.23065>
- Cozzuol, M.A. (2006) The Acre vertebrate fauna: age, diversity, and geography. *Journal of South American Earth Sciences*, 21, 185–203.  
<https://doi.org/10.1016/j.jsames.2006.03.005>
- Dodson, P. (1975) Functional and ecological significance of relative growth in *Alligator*. *Journal of Zoology*, 175, 315–355.  
<https://doi.org/10.1111/j.1469-7998.1975.tb01405.x>
- Duarte, K.S. (2011) Levantamentos Exploratórios da ANP na Bacia do Acre. *Revista Técnico-Científica da ANP*, 1, 4–33.
- Fedo, C.M., Sircombe, K.N. & Rainbird, R.H. (2003) Detrital Zircon Analysis of the Sedimentary Record. *Reviews in Mineralogy and Geochemistry*, 53 (1), 277–303.  
<https://doi.org/10.2113/0530277>
- Fitzhugh, K. (2016) Sequence Data, Phylogenetic Inference, and Implications of Downward Causation. *Acta Biotheoretica*, 64(2), 133–160.  
<https://doi.org/10.1007/s10441-016-9277-0>
- Fortier, D.C., Souza-Filho, J.P., Guilherme, E., Maciente, A.A.R. & Schultz, C.L. (2014) A new specimen of *Caiman brevirostris* (Crocodylia, Alligatoridae) from the late Miocene of Brazil. *Journal of Vertebrate Paleontology*, 34 (4), 820–834.  
<https://doi.org/10.1080/02724634.2014.838173>
- Foth, C., Bona, P. & Desojo, J.B. (2015) Intraspecific variation in the skull morphology of black caiman *Melanosuchus niger* (Alligatoridae, Caimaninae). *Acta Zoologica*, 96, 1–13.  
<https://doi.org/10.1111/azo.12045>
- Foth, C., Fernandez-Blanco, M.V., Bona, P. & Scheyer, T.M. (2017) Cranial shape variation in jacarean caimanines (Crocodylia, Alligatoroidea) and its implications in the taxonomic status of extinct species: the case of *Melanosuchus fisheri*. *Journal of Morphology*, 279 (2), 259–273.  
<https://doi.org/10.1002/jmor.20769>
- Gasparini, Z. (1968) Nuevos restos de *Rhamphostomopsis neogaeus* (Burm.) Rusconi, 1933, (Reptilia, Crocodylia) del “Mesopotamiense” (Plioceno medio-superior) de Argentina. *Ameghiniana*, 5, 299–311.
- Gauthier, J.A., Kearney, M., Maisano, J.A., Rieppel, O. & Behlke, A.D.B. (2012) Assembling the squamate tree of life: perspectives from the phenotype and the fossil record. *Bulletin of the Peabody Museum of Natural History*, 53 (1), 3–308.  
<https://doi.org/10.3374/014.053.0101>
- Gervais, P. (1876) Crocodile gigantesque fossile au Brésil. *Journal de Zoologie*, 5, 232–236.
- Grigg, G. & Kirshner, D. (2015) *Biology and evolution of crocodylians*. Csiro Publishing, Claytown South, 672 pp.
- Goloboff, P.A. & Catalano, S.A. (2016) TNT version 1.5, including a full implementation of phylogenetic morphometrics. *Cladistics*, 32 (3), 221–238.

<https://doi.org/10.1111/cla.12160>

- Gray, J.E. (1862) A synopsis of the species of Alligators. *Annals and magazine of natural history*, 10 (3), 125–169.
- Guilherme, E., Bocquentin, J. & Porto, A.L. (2011) A New specimen of the genus *Octodontobradys* (Orophodontidae, Octodontobradynae) from the Late Miocene-Pliocene of the southwestern Amazon Basin, Brazil. *Anuário do Instituto de Geociências—UFRJ*, 34 (2), 38–45.  
[https://doi.org/10.11137/2011\\_2\\_38-45](https://doi.org/10.11137/2011_2_38-45)
- Gürich, G. (1912) *Gryposuchus jessei*, ein neues schmalschmauziges KroKodile aus dens jüngeren Ablagerungen des oberen Amazonas-Gebietes. *Jahrbuch der Hamburgischen Wissenschaftlichen Aulalten*, 29, 59–71.
- Haag, N.A. & Henriques, M.H. (2016) The paleontological heritage of the Acre (Amazonia, Brazil): contribution towards a national paleontological database. *Geoheritage*, 8, 381–391.  
<https://doi.org/10.1007/s12371-015-0163-y>
- Hammer, Ø. & Harper, D.A.T. (2008) *Paleontological data analysis*. John Wiley & Sons, Hoboken, New Jersey, 368 pp.
- Hammer, Ø., Harper, D.A.T. & Ryan, P.D. (2001) PAST: Paleontological statistics software package for education and data analysis. *Palaeontologia Electronica*, 4 (1), 1–9.
- Hastings, A.K., Reisser, M. & Scheyer, T.M. (2016) Character evolution and the origin of Caimaninae (Crocodylia) in the New World Tropics: new evidence from the Miocene of Panama and Venezuela. *Journal of Paleontology*, 90 (2), 317–332.  
<https://doi.org/10.1017/jpa.2016.37>
- Herron, J.C. (1994) Body Size, Spatial Distribution, and Microhabitat Use in the Caimans, *Melanosuchus niger* and *Caiman crocodilus*, in a Peruvian Lake. *Journal of Herpetology*, 28 (4), 508–513.  
<https://doi.org/10.2307/1564969>
- Hsiou, A.S. & Albino, A.M. (2009) Presence of the genus *Eunectes* (Serpentes, Boidae) in the Neogene of Southwestern Amazonia, Brazil. *Journal of Herpetology*, 43, 612–619.  
<https://doi.org/10.1670/08-295.1>
- Hsiou, A.S., Albino, A.M. & Ferigolo, J. (2009) First Lizard Remains (Teiidae) From The Miocene of Brazil (Solimões Formation). *Revista Brasileira de Paleontologia*, 12 (3), 225–230.  
<https://doi.org/10.4072/rbp.2009.3.05>
- Hsiou, A.S., Albino, A.M. & Ferigolo, J. (2010) Reappraisal of the South American Miocene snakes of the genus *Colombophis*, with description of a new species. *Acta Palaeontologica Polonica*, 55, 365–379.  
<https://doi.org/10.4202/app.2009.1111>
- Hoogmoed, M.S. & Gruber, U. (1983) Spix and Wagler type specimens of reptiles and amphibians in the Natural History Museum in Munich (Germany) and Leiden (The Netherlands). *Spixiana*, 9, 319–415.
- Hoorn, C., Bogotá-A, G.R., Romero-Baez, M., Lammertsma, E.I., Flantua, S.G.A., Dantas, E.L., Dino, R., Carmo, D.A. & Cheemale Jr., F. (2017) The Amazon at sea: Onset and stages of the Amazon River from a marine record, with special reference to Neogene plant turnover in the drainage basin. *Global and Planetary Change*, 153, 51–65.  
<https://doi.org/10.1016/j.gloplacha.2017.02.005>
- Hoorn, C., Wesselingh, F.P., Ter Steege, H., Bermúdez, M.A., Mora, A., Sevink, J., Sanmartín, I., Sánchez-Mesenguer, A., Anderson, C.L., Figueiredo, J.P., Jaramillo, C., Riff, D., Negri, F.R., Hooghiemstra, H., Lundberg, J., Stadler, T., Särkinen, T. & Antonelli, A. (2010) Amazonia Through Time: Andean Uplift, Climate Change, Landscape Evolution, and Biodiversity. *Science*, 330, 927–931.  
<https://doi.org/10.1126/science.1194585>
- Horbe, A.M.C., Roddaz, M., Gomes, L.B., Castro, R.T., Dantas, E.L. & Carmo, D.A. (2019) Provenance of the Neogene sediments from the Solimões Formation (Solimões and Acre Basins), Brazil. *Journal of South American Earth Sciences*, 93, 232–241.  
<https://doi.org/10.1016/j.jsames.2019.05.004>
- Iordansky, N.N. (1973) The skull of the Crocodilia. In: Gans, C. & Parsons, T. (Eds.), *Biology of the Reptilia*. Vol. 4. Academic Press, London, pp. 50–68.
- Jackson, D.A. (1993) Stopping Rules in Principal Components Analysis: A Comparison of Heuristical and Statistical Approaches. *Ecology*, 74 (8), 2204–2214.  
<https://doi.org/10.2307/1939574>
- Jollie, M.T. (1960) The head skeleton of the lizard. *Acta Zoologica*, 41 (1–2), 1–64.  
<https://doi.org/10.1111/j.1463-6395.1960.tb00474.x>
- Kerber, L., Negri, F.R., Ribeiro, A.M., Nasif, N., Souza-Filho, J.P. & Ferigolo, J. (2017) Tropical Fossil Caviomorph Rodents from the Southwestern Brazilian Amazonia in the Context of the South American Faunas: Systematics, Biochronology, and Paleobiogeography. *Journal of Mammal Evolution*, 24, 57–70.  
<https://doi.org/10.1007/s10914-016-9340-2>
- Kerber, L., Negri, F.R., Ribeiro, A.M., Vucetich, M.G. & Souza-Filho, J.P. (2016). Late Miocene potamarchine rodents from southwestern Amazonia, Brazil—with description of new taxa. *Acta Palaeontologica Polonica*, 61 (1), 191–203.  
<https://doi.org/10.4202/app.00091.2014>
- Klingenberg, C.P. (2013) Visualizations in geometric morphometrics: how to read and how to make graphs showing shape changes. *Hystrix, the Italian Journal of Mammalogy*, 24 (1), 15–24.  
<https://doi.org/10.4404/hystrix-24.1-7691>

- Lacerda, M.B.S., Souza, L.G., Lobo, L.S., Schaefer, C.E.G.R. & Romano, P.S.R. (2020) New outcrop with vertebrate remains from Solimões Formation (Eocene-Pliocene), Southern Solimões Basin, Acre State, Northern Brazil. *Journal of South American Earth Sciences*, 101, 102588.  
<https://doi.org/10.1016/j.jsames.2020.102588>
- Lacerda, M.B.S., Souza, R.G. & Romano, P.S.R. (2018) The systematic potential of morphology and geometric morphometrics of tibia proximal articulation in Caimaninae (Alligatoroidea). In: Boletim de Resumos. *XI Simpósio Brasileiro de Paleontologia de Vertebrados*, 2018, pp. 57.
- Langston, W. (1965) Fossil crocodilian from Colombia and the Cenozoic history of the Crocodylia in South America. *University of California Publications in Geological Sciences*, 52, 1–157.
- Langston, W. & Gasparini, Z. (1997) Crocodilians, *Gryposuchus*, and the South Americans gavials. In: Kay, R.F., Madden, R.H., Cifelli, R.L. & Flynn, J.J. (Eds.), *Vertebrate Paleontology in the Neotropics: The Miocene Fauna of La Venta, Colombia*. Smithsonian Institution, Washington, pp. 113–154.
- Latrubesse, E.M., Bocquentin, J., Santos, C.R. & Ramonell, C.G. (1997) Paleoenvironmental model for the late Cenozoic southwestern Amazonia paleontology and geology. *Acta Amazônica*, 27, 103–118.  
<https://doi.org/10.1590/1809-43921997272118>
- Latrubesse, E.M., Cozzuol, M., Silva-Caminha, S.A.F., Rigsby, C.A., Absy, M.L. & Jaramillo, C. (2010) The Late Miocene paleogeography of the Amazon Basin and the evolution of the Amazon River system. *Earth-Science Reviews*, 99, 99–124.  
<https://doi.org/10.1016/j.earscirev.2010.02.005>
- Latrubesse, E., Silva, S.A., Cozzuol, M. & Absy, M.L. (2007) Late Miocene continental sedimentation in southwestern Amazônia and its regional significance: biotic and geological evidence. *Journal of South American Earth Sciences*, 23 (1), 61–80.  
<https://doi.org/10.1016/j.jsames.2006.09.021>
- Maddison, W.P. & Maddison, D.R. (2015) Mesquite: a modular system for evolutionary analysis. Version 3.03. Available from: <http://mesquiteproject.org> (accessed 25 November 2020)
- Magnusson, W.E. (1985) Habitat selection, parasites and injuries in Amazonian crocodilians. *Amazoniana*, 9, 193–204.
- Magnusson, W.E., Silva, E.V. & Lima, A.P. (1987) Diets of Amazonian crocodilians. *Journal of Herpetology*, 21 (2), 85–95.  
<https://doi.org/10.2307/1564468>
- Marioni, B., Silveira, R., Magnusson, W.E. & Thorbjarnarson, J. (2008) Feeding Behavior of Two Sympatric Caiman Species, *Melanosuchus niger* and *Caiman crocodilus*, in the Brazilian Amazon. *Journal of Herpetology*, 42 (4), 768–772.
- Medem, F. (1963) Osteología Craneal, Distribución geográfica y ecología de *Melanosuchus niger* (Spix) (Crocodylia, Alligatoridae). *Revista de la Academia Colombiana de Ciencias Exactas, Físicas y Naturales*, 12 (45), 5–23.  
<https://doi.org/10.1590/S0100-736X2016001000018>
- Medina, C.J. (1976) Crocodilians from the Late Tertiary of Northwestern Venezuela: *Melanosuchus fisheri* sp. nov.. *Breviora*, 438, 1–14.
- Monteiro, L.R. (2013) Morphometrics and the comparative method: studying the evolution of biological shape. *Hystrix, the Italian Journal of Mammalogy*, 24 (1), 25–32.  
<https://doi.org/10.4404/hystrix-24.1-6282>
- Morrone, J.J. (2013) Cladistic biogeography of the Neotropical region: identifying the main events in the diversification of the terrestrial biota. *Cladistics*, 30 (2), 202–214.  
<https://doi.org/10.1111/cla.12039>
- Mook, C.C. (1921) Skull characters of Recent Crocodilia, with notes on the affinities of the Recent genera. *Bulletin of American Museum of Natural History*, 44 (13), 123–268.
- Negri, F.R., Bocquentin-Villanueva, J., Ferigolo, J. & Antoine, P.O. (2010) A Review of Tertiary mammal faunas and birds from western Amazonia. In: Hoorn, C. & Wesselingh, F. P. (Eds.), *Amazonia: Landscape and Species Evolution: A Look into the Past*. Wiley-Blackwell, Oxford, pp. 245–258.
- Norell, M.A., Clark, J.M. & Hutchison, J.H. (1994) The Late Cretaceous Alligatoroid *Brachychampsia montana* (Crocodylia): new material and putative relationships. *American museum novitates*, 3116, 1–26.
- Oaks, J.R. (2011) A time-calibrated species tree of Crocodylia reveals a recent radiation of the true crocodiles. *Evolution*, 65 (11), 3285–3297.  
<https://doi.org/10.1111/j.1558-5646.2011.01373.x>
- Poe, S. (1996) Data set incongruence and the phylogeny of Crocodilians. *Systematic Biology*, 45 (4), 393–414.  
<https://doi.org/10.1093/sysbio/45.4.393>
- Pooley, A.C. & Gans, C. (1976) The Nile crocodile. *Scientific American*, 234 (4), 114–125.
- Price, L.I. (1967) Sobre a mandíbula de um gigantesco crocodilídeo extinto do alto Rio Juruá, Estado do Acre. In: Lent, H. (Eds.), *Atas Simpósio sobre a Biota Amazônica (Geociências)*. Sociedade Brasileira de Paleontologia, Belém, pp. 359–371.
- Price, L.I. (1964) Sobre o crânio de um grande crocodilídeo extinto do Alto de Rio Juruá, Estado do Acre. *Anais da Academia Brasileira de Ciências*, 56, 59–66.
- Price, L.I., Campos, D.A. & Campos, D.R.B. (1977) Localidades fossilíferas das Folhas SB.18 Javari e SC.18 Contamana. In: Barros, A.M., Alvez, E.D.O., Araujo, J.F.V., Lima, M.I.C. & Fernandes, C.A.C (Eds.), (Geologia). Projeto RadamBrasil, Rio de Janeiro, Levantamento de recursos naturais 13, pp. 17–103.
- Rancy, A. (1985) Estudos de paleovertebrados na Amazônia Ocidental. *Coletânea Trabalhos Paleontológicos MME-DNPM, Série Geol*, 27, 99–103.



- Ribeiro, A.M., Madden, R.H., Negri, F.R., Kerber, L., Hsiou, A.S., Rodrigues, K.A. (2013) Mamíferos fósiles y biocronología en el suroeste de la Amazonia, Brazil. In: Brandoni, D. & Noriega, J.I. (Eds.), *El neógeno de la Mesopotamia Argentina. Asociación Paleontológica Argentina Publicación Especial 14*. Asociación Paleontológica Argentina, Buenos Aires, pp. 207–221.
- Rieppel, O. (1993) Studies on skeleton formation in reptiles. V. Patterns of ossification in the skeleton of *Alligator mississippiensis* Daudin (Reptilia, Crocodylia). *Zoological Journal of the Linnean Society*, 109 (3), 301–325.  
<https://doi.org/10.1111/j.1096-3642.1993.tb02537.x>
- Riff, D. & Aguilera, O.A. (2008) The world's largest gharials *Gryposuchus*: Description of *G. croizati* n. sp. (Crocodylia, Gavialidae) from the Upper Miocene Urumaco Formation, Venezuela. *Paläontologische Zeitschrift*, 82, 178–195.  
<https://doi.org/10.1007/BF02988408>
- Riff, D., Romano, P.S.R., Oliveira, G.R. & Aguilera, O.A. (2010) Neogene Crocodile and Turtle Fauna in Northern South America. In: Hoorn, C. & Wesselingh, F. (Eds.), *Amazonia, Landscape and Species Evolution: A Look into the Past*. Wiley-Blackwell, London, pp. 259–280.
- Roberto, J.I., Bittencourt, P.S., Muniz, F.L., Hernández-Rangel, S.M., Nóbrega, Y.C., Ávila, R.W., Souza, B.C., Alvarez, G., Miranda-Chumacero, G., Campos, Z., Farias, I.P. & Hrbek, T. (2020) Unexpected but unsurprising lineage diversity within the most widespread Neotropical crocodilian genus *Caiman* (Crocodylia, Alligatoridae). *Systematics and Biodiversity*, 18 (4), 377–395.  
<https://doi.org/10.1080/14772000.2020.1769222>
- Rohlf, F.J. (2015) The tps series of software. *Hystrix, the Italian Journal of Mammalogy*, 26 (1), 9–12.  
<https://doi.org/10.4404/hystrix-26.1-11264>
- Rueda-Almonacid, J.V., Carr, J.L., Mittermeier, R.A., Rodríguez-Mahecha, J.V., Mast, R.B., Vogt, R.C., Rhodin, A.G., Ossa-Velásquez, J., Rueda, J.N. & Mittermeier, C.G. (2007) *Las tortugas y los cocodrilianos de los países andinos del trópico. Serie de guías tropicales de campo*, 6. Conservación Internacional. Editorial Panamericana, Formas e Impressos, Bogotá, 537 pp.
- Salas-Gismondi, R., Flynn, J.J., Baby, P., Tejada-Lara, J.V., Wesselingh, F.P. & Antoine, P.-O. (2015) A Miocene hyperdiverse crocodilian community reveals peculiar trophic dynamics in proto-Amazonian mega wetlands. *Proceedings of the Royal Society*, 282 (1804), 20142490.  
<https://doi.org/10.1098/rspb.2014.2490>
- Scheyer, T.M., Aguilera, O.A., Delfino, M., Fortier, D.C., Carlini, A.A., Sánchez, R., Carrillo-Briceño, J.D., Quiroz, L. & Sánchez-Villagra, M.R. (2013) Crocodylian diversity peak and extinction in the late Cenozoic of the northern Neotropics. *Nature Communications*, 4 (1), 1–9.  
<https://doi.org/10.1038/ncomms2940>
- Scheyer, T.M. & Delfino, M. (2016) The late Miocene caimanine fauna (Crocodylia: Alligatoroidea) of the Urumaco Formation, Venezuela. *Palaeontologia Electronica*, 19(3), 1–57.  
<https://doi.org/10.5167/uzh-129827>
- Scheyer, T.M., Hutchinson, J.R., Strauss, O., Delfino, M., Carrillo-Briceño, J.D., Sánchez, R., Sánchez-Villagra, M.R. (2019) Giant extinct caiman breaks constraint on the axial skeleton of extant crocodylians. *eLife*, 8, e49972.  
<https://doi.org/10.7554/eLife.49972>
- Scheyer, T.M. & Moreno-Bernal, J.W. (2010) Fossil crocodylians from Venezuela in the context of South American faunas. In: Sánchez-Villagra, M.R., Aguilera, O.A. & Carlini, A.A. (Eds.), *Urumaco and Venezuelan Palaeontology—The Fossil Record of the Northern Neotropics*. Indiana University Press, Bloomington, pp. 192–213.
- Silveira, R., Magnusson, W.E. & Campos, Z. (1997) Monitoring the Distribution, Abundance and Breeding Areas of *Caiman crocodilus crocodilus* and *Melanosuchus niger* in the Anavilhanas Archipelago, Central Amazonia, Brazil. *Journal of Herpetology*, 31 (4), 514–520.
- Slize, D.E. (2007) Geometric Morphometrics. *Annual Review of Anthropology*, 36, 261–281.  
<https://doi.org/10.1146/annurev.anthro.34.081804.120613>
- Souza, R.G., Cidade, G.M., Campos, D.A. & Riff, D. (2016) New Crocodylian remains from the Solimões Formation (Upper Miocene), State of Acre, Northwestern Brazil and their significance. *Revista Brasileira de Paleontologia*, 19 (2), 217–232.  
<https://doi.org/10.4072/rbp.2016.2.06>
- Souza-Filho, J.P. (1987) *Caiman brevirostris* sp. nov., um novo Alligatoridae da Formação Solimões (Pleistoceno) do Estado do Acre, Brasil. In: *Anais do X Congresso Brasileiro de Paleontologia, Rio de Janeiro*, 1987, pp. 173–180.
- Souza-Filho, J.P. (1993). Ocorrência de *Charactosuchus fieldsi* e *Charactosuchus* n. sp. (Crocodylia, Crocodylidae) no Neógeno da Amazônia brasileira. *Ameghiniana*, 30 (1), 113.
- Souza-Filho, J.P., Negri, F.R. & Guilherme, E. (2014) Extinção de Crocodyliformes na Região Sul Ocidental da Amazônia (Acre-Brasil) e Norte da América do Sul (FM Urumaco-Venezuela): Evidência de variações climáticas no Neógeno da América do Sul. In: Carvalho, I.S., Garcia, M.J., Lana, C.C. & Strohschoen Jr., O. (Eds.), *Paleontologia: Cenários de Vida—Paleoclima. Vol. 5*. Editora Interciência, Rio de Janeiro, pp. 317–325.
- Souza-Filho, J.P., Souza, R.G., Hsiou, A.S., Riff, D., Guilherme, E., Negri, F.R. & Cidade, G.M. (2019) A new caimanine (Crocodylia, Alligatoroidea) species from the Solimões Formation of Brazil and the phylogeny of Caimaninae. *Journal of Vertebrate Paleontology*, 38 (5), e1528450.

<https://doi.org/10.1080/02724634.2018.1528450>

- Souza-Filho, J.P. & Bocquentin-Villanueva, J.C. (1989) *Brasilosuchus mendesi*, n. g., n. sp., um novo representante da Família Gavialidae do Neógeno do Acre, Brasil. In: *Anais do XI Congresso Brasileiro de Paleontologia, Curitiba*, 1989, pp. 457–463.
- Souza-Filho, J.P. & Guilherme, E. (2015) A Paleontologia no Estado do Acre. In Adamy, A. (Eds.), *Geodiversidade do Estado do Acre: Programa Geologia do Brasil, Levantamento da Geodiversidade*. Ministério de Minas e Energia, CPRM—Serviço Geológico do Brasil, Porto Velho, pp. 145–158.
- Spix, J.B. (1825) Animalia nova sive species novae Lacertarum, quas in itinere per Brasiliam annis MDCCCXVII-MDCCCXX jussu et auspiciis Maximiliani Josephi I. In: De Pix, D.J.B. (Eds.), *Bavaria Regis suscepto collegit et descripsit*. Typis, Franc. Seraph. Hübschamanni, Munich, pp. 1–110.
- Starck, D. & Anzotequi, L.M. (2001) The late Miocene climatic change—Persistence of a climatic signal through the orogenic stratigraphic record in northwestern Argentina. *Journal of South American Earth Sciences*, 14 (7), 763–774.  
[https://doi.org/10.1016/S0895-9811\(01\)00066-9](https://doi.org/10.1016/S0895-9811(01)00066-9)
- Thorbjarnarson, J.B. (2010) Black Caiman *Melanosuchus niger*. In: Manolis, S.C. & Stevenson, C. (Eds.), *Crocodyles. Status Survey and Conservation Action Plan 3ed*. Crocodile Specialist Group, Darwin, pp. 29–39.
- Vieira, L.G., Santos, A.L.Q., Lima, F.C., Mendonça, S.H.S.T., Menezes, L.T. & Sebben, A. (2016) Osteologia de *Melanosuchus niger* (Crocodylia: Alligatoridae) e a evidência evolutiva. *Pesquisa Veterinária Brasileira*, 36 (10), 1025–1044.  
<https://doi.org/10.1590/s0100-736x2016001000018>
- Webster, M. & Sheets, H.D. (2010) A practical introduction to landmark-based geometric morphometrics. In: Alroy, J. & Hunt, G. (Eds.), *Quantitative Methods in Paleobiology. The Paleontological Society Papers*, 16, pp. 163–188.
- Zelditch, M.A., Swiderski, D.L. & Sheets, H.D. (2012) *Geometric morphometrics for biologists: a primer*. Academic Press, Cambridge, 488 pp.

## List of Supporting Information

**Supporting Information 1 (SI 1)** TNT output; and Geometric Morphometrics Methods.

**Supporting Information 2 (SI 2)** Data Matrix (morphological characters, .tnt extension).

**Supporting Information 3 (SI 3)** Minimum-Length Trees (MLT, .tre extension).

**Supporting Information 4 (SI 4)** List of Morphological Characters.